

Lehrstuhl für Informatik 10 (Systemsimulation)



Simulation of a solar airship

Armin Bundle

Master thesis

Simulation of a solar airship

Armin Bundle

Master thesis

Aufgabensteller: Prof. Dr. C. Pflaum

Betreuer: Prof. Dr. C. Pflaum

Bearbeitungszeitraum: 1.7.2017 – 2.1.2018

Erklärung:

Ich versichere, dass ich die Arbeit ohne fremde Hilfe und ohne Benutzung anderer als der angegebenen Quellen angefertigt habe und dass die Arbeit in gleicher oder ähnlicher Form noch keiner anderen Prüfungsbehörde vorgelegen hat und von dieser als Teil einer Prüfungsleistung angenommen wurde. Alle Ausführungen, die wörtlich oder sinngemäß übernommen wurden, sind als solche gekennzeichnet.

Der Universität Erlangen-Nürnberg, vertreten durch den Lehrstuhl für Systemsimulation (Informatik 10), wird für Zwecke der Forschung und Lehre ein einfaches, kostenloses, zeitlich und örtlich unbeschränktes Nutzungsrecht an den Arbeitsergebnissen der Masterthesis einschließlich etwaiger Schutzrechte und Urheberrechte eingeräumt.

Erlangen, den 2. Januar 2018

.....

Abstract

The present Master thesis 'Simulation of a solar airship' describes the simulation of two types of solar airship. The first type is a rigid airship similar to the airship LZ 129, called 'Hindenburg', the second type is alike the Zeppelin NT semi-rigid airship.

For both types the physically basic, the buoyancy force and the force of gravity for the vertical movement as well as the thrust force and the drag force for the horizontal movement were examined. For the calculations of the flight dynamics a new algorithm was designed for the 'Hindenburg' and the Zeppelin NT.

The first step is the calculation of the possible provided electrical energy by the airships solar cell field under the condition of arbitrary flight levels, locations and times of the day/year. The generated power is used to calculate the airships thrust in relation to the engines efficiency. The thesis presents an algorithm to calculate the efficiency of the engines by taking e.g. the flight altitude, the number of engines and the propellor size into account. Based on the calculated efficiency values it is possible to compare these with real efficiency values of the 'Hindenburg' and the Zeppelin NT. Using these calculations it was possible to compare the flight dynamics properties of the 'Hindenburg' and the Zeppelin NT.

The following simulations were executed with construction properties and input parameter of the Zeppelin NT. For a more accurate simulation real weather data from the past were considered. In addition the accomplished airship velocities for different altitude were examined. Finally airship flights on different locations and different season were simulated and analyzed.

I Table of contents

I	Table of contents	II
II	List of Figures	IV
III	List of Tables	V
1	Introduction	1
2	Basic equations	1
3	Drag force	2
4	Physical air properties	3
5	The different airship construction methods	4
6	The airship buoyancy	5
7	The center of mass	6
8	Sun radiation at the airship	7
8.1	The different kinds of sunlight	7
8.2	Solar constant	7
8.3	Solar Time	8
8.4	Solar altitude	9
8.5	Direct clear-sky radiation	10
8.6	Diffuse clear-sky radiation	12
8.7	Ground reflected radiation	12
9	The discretization of the airship	13
9.1	The geometry as an ellipsoid	13
9.2	The solar azimuth angle	15
9.3	The power generation of the airship surface	16
10	The Engine of the airship	17
11	Geographic coordinates	21
12	Weather data	22
12.1	Access on the weather data	23
12.2	Wind data	25
13	Analytical formula for the airship velocity	27
14	Value settings of the simulated airships	29

15 Requirement checks	29
15.1 The buoyancy and maximum altitude of the airships	29
15.2 Results of center of mass check	32
16 Simulation results	32
16.1 Comparing the 'Hindenburg' and the Zeppelin NT	33
16.2 The influence of the wind on the airship	33
16.3 The influence of the altitude on the airships velocity	35
16.4 Simulation results for different seasons and locations	37
17 Conclusion and future work	40
A Input parameter for the evaluation of the efficiency of the engines	I
B Additional data for the buoyancy of the airships	I
C Additional weather data simulation results	II
D Literature	VII

II List of Figures

Fig. 1	The change of air properties by altitude.	4
Fig. 2	The 'Hindenburg' rigid airship.	5
Fig. 3	The zeppelin NT semi-rigid airship.	5
Fig. 4	Variation of extraterrestrial solar radiation as a function of time of year [5].	7
Fig. 5	The equation of time E in minutes as a function of time of year [5]. . .	8
Fig. 6	The power of the sun radiation depending on altitude.	12
Fig. 7	The sun azimuth angle [18].	15
Fig. 8	Cross-section of a propellor engine and the corresponding velocities. . .	18
Fig. 9	Variation of theoretical efficiency.	21
Fig. 10	The airships mass by maximal altitude.	30
Fig. 11	The velocity of the airship depending on its mass.	31
Fig. 12	Comparison between the 'Hindenburg' and the Zeppelin NT.	33
Fig. 13	The influence of the wind at the airship.	34
Fig. 14	The wind velocity on the route.	35
Fig. 15	The velocity of the Zeppelin NT on different altitude.	36
Fig. 16	The generated power of the Zeppelin NT on different altitude.	36
Fig. 17	The airship velocity on flights with 1 km altitude on different locations. .	37
Fig. 18	The generated power on flights with 1 km altitude on different locations. .	38
Fig. 19	The airships velocities on flights with 6 km altitude on different locations. .	39
Fig. 20	The generated power on flight with 6 km altitude on different locations. .	40
Fig. 21	The influence of the wind on the airship.	II
Fig. 22	The influence of the wind on the airship.	II
Fig. 23	The influence of the wind on the airship.	III
Fig. 24	The influence of the wind on the airship.	III
Fig. 25	Wind data at noon 01/06/12.	IV
Fig. 26	Wind data at noon 01/07/12.	IV
Fig. 27	Wind data at noon 01/08/12.	V
Fig. 28	Pressure and temperature at noon 01/06/12.	V
Fig. 29	Pressure and temperature at noon 01/07/12.	VI
Fig. 30	Pressure and temperature at noon 01/08/12.	VI

III List of Tables

Tab. 1	Variation of Reynolds number depending on the thickness ratio [10]. . .	3
Tab. 2	Day of the year after the spring equinox.	10
Tab. 3	Correction factors for climate types [16].	11
Tab. 4	Albedo values for certain surfaces [15] [14].	13
Tab. 5	The efficiency of the 'Hindenburg' and the Zeppelin NT.	28
Tab. 6	Specification of the 'Hindenburg' and the Zeppelin NT airship.	29
Tab. 7	Input parameter for the simulated flights.	29
Tab. 8	Parameter for an airship with solar cells on the top half of the hull. . .	31
Tab. 9	Parameter for an airship with the hull totally covered in solar cells. . .	31
Tab. 10	Results and input parameter of the center of gravity evaluation.	32
Tab. 11	Results of the Zeppelin NT flight on different altitude.	37
Tab. 12	Results of the Zeppelin NT on flights with 1 km altitude on different locations.	38
Tab. 13	Results of the Zeppelin NT on flights with 1 km altitude on different locations.	39
Tab. 14	Parameter for the efficiency of the engine.	I
Tab. 15	Remaining masses for various maximum altitude.	I

1 Introduction

The history of the professional using of airship goes back for approximately 100 years. One of the main reasons for the development of airships at the beginning of the 19th century was the military usage in the First World War [1]. The climax of the first area was reached by manufacturing in 1936 the airship LZ 129 called 'Hindenburg' the largest aircraft ever built. The end of the first area came abruptly by the 'Hindenburg disaster' where the airship burned down because of hydrogen as lifting gas. After a few years the construction methods advanced and semi-rigid airships respectively blimps are mostly built.

Over the past years the needs on aircrafts changed. With decreasing resources and global warming a more environmental friendly way of traveling would be welcome. The idea is to use solar energy to perform the airship. The advantage over an airplane would be no kerosene consumption, no pollutant emissions and no noise pollution. An evidently disadvantage is the lower velocity of a solar airship and the possible dependency on weather conditions.

On the other hand a solar airship can possibly operate in other fields, in difference to an airplane. Thinkable are missions in regions without available airport environment and equipment. Other areas of use may be long term surveillance with manned or unmanned airships, of huge areas like offshore wind farms, pipes or waterways. The discussed points before bring the desired requirements for a fictitious solar airship.

In this thesis performance capability of the flight dynamics of a solar airships should be calculated with computer simulation.

2 Basic equations

The general approach is by using Newton's second law of motion. It defines the relation between the force F and the mass m of an object and its acceleration a and is listed in in the following.

$$F = ma \quad (1)$$

The object is in this case the whole airship. The force which accelerates the airship is the thrust F_{thrust} . The opponent is the drag force F_{drag} that slows down the acceleration. The real force applied on the airship can be calculated by subtracting these (compare equation 2).

$$F = F_{thrust} - F_{drag} \quad (2)$$

Inserted into equation 1 brings the desired equation 3, where the acceleration is equal to the derivative of the velocity.

$$a = \dot{v} = \frac{F_{thrust} - F_{drag}}{m} \quad (3)$$

The value of velocity for a time step can be determined by the current velocity value in addition with the change Δv on it. The change of the velocity is equal to the derivative of the velocity times the time interval h . This differential equation is calculated with the explicit euler method (compare equation 5).

$$v_{n+1} = v_n + \Delta v = v_n + h\dot{v} \quad (4)$$

The now known velocity is used to update the position of the airship which is presented the following.

$$x_{n+1} = x_n + hv \quad (5)$$

3 Drag force

The general formula of the drag force for an arbitrary object is listed in equation 6 [2]. It stands out, that the drag force depends on the air density ρ . F_{drag} decreases with higher altitude. Furthermore the velocity of the airship v as a square leads to disproportional higher forces for rising velocities.

$$F_{drag} = \frac{1}{2} \rho v^2 A_s c_w \quad (6)$$

For each airship the surface area A_s and the drag coefficient c_w has to be estimated. It is a common practice to calculate the surface area of an airship in terms of the envelopes volume V as shown in equation 7 [3].

$$A_s = V^{\frac{2}{3}} \quad (7)$$

The drag coefficient highly depends on the airships hull shape. [3] suggests a calculation in terms of the Reynolds number Re , the length l and the maximum diameter d of the airship and is listed in the following equation.

$$c_w = \left[0.172 \left(\frac{l}{d} \right)^{\frac{1}{3}} + 0.252 \left(\frac{d}{l} \right)^{1.2} + 1.032 \left(\frac{d}{l} \right)^{2.7} \right] \cdot \frac{1}{Re^{\frac{1}{6}}} \quad (8)$$

Table 1 shows Reynolds number for ellipsoids of different length to diameter ratios. The division of the airships maximum diameter and length is called thickness ratio.

Table 1: Variation of Reynolds number depending on the thickness ratio [10].

d/l	Reynolds number
0.15	1.138
0.18	1.000
0.20	0.940

4 Physical air properties

The drag force depends on air density. It changes by the altitude. The Barometric formula describes the air density depending on the air pressure and the air temperature. Equation 9 points out the air density ρ depending on molar mass of Earth's air M , the universal gas constant R , the temperature T and the air pressure p [4].

$$\rho(h) = \frac{p(h)M}{RT(h)} \quad (9)$$

The air pressure (compare equation 10) and the air temperature (compare equation 11) also depends on the altitude.

To calculate the pressure p , the value of it on sea level p_0 is needed as well as the temperature T , the standard temperature laps rate L_b and the altitude h itself.

$$p(h) = 100p_0 \left[1 - \frac{L_b * h}{T(h)} \right]^{5.255} \quad (10)$$

The temperatur T (compare equation 11) couples the temperature gradient $\frac{dT}{dh}$ which is listed in equation 12 and the ground temperature T_0 [13].

$$T(h) = T_0 - \frac{dT}{dh}h \quad (11)$$

$$\frac{dT}{dh} = \begin{cases} 0.0098, & \text{h smaller 2000m} \\ 0.0065, & \text{else} \end{cases} \quad (12)$$

A plot of the calculated density and temperature values is shown in Figure 1. The ordinate records altitude from 0 to 10 kilometer.

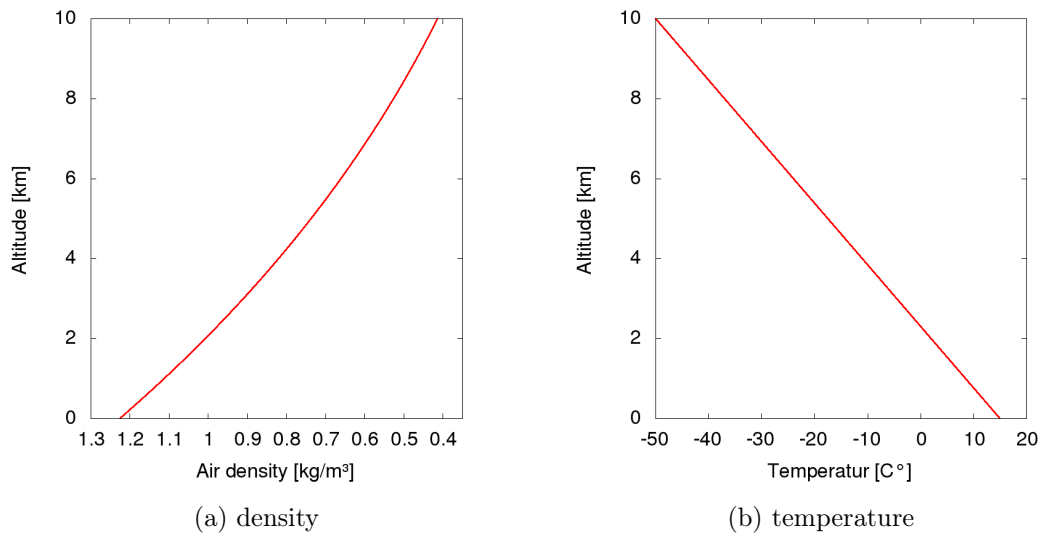


Figure 1: The change of air properties by altitude.

5 The different airship construction methods

There are three main construction methods for airships. A Rigid airship has a frame with a skin which is surrounding the gas. If the gas drains the rigid airship stays in shape. These architectures are only build in the beginning of the airship ages, before the end of the Second World War. The most famous example was the airship LZ 129, better known as 'Hindenburg', which is shown in Figure 2.

The other, so called blimp has no solid structure inside the hull, therefore the envelope collapse when the gas escapes. A blimp needs a constant pressure inside the envelope to stay in shape. A third construction method is a combination of a blimp and a rigid airship called semi-rigid airship. An example is the Zeppelin NT airship which is shown in Figure 3.

Blimps and semi-rigid airships contain ballonets to keep the pressure constant inside the envelope. The ballonets are inflated with air while rising from the ground. When the airship rises, air drains through valves out of the ballonets respectively airship in order to keep the pressure constant. This implies that the ballonets are empty on maximum flight altitude.

One big advantage of semi-rigid airships is the additional safety. Even when the envelope is collapsing by a pressure loss the semi-rigid structure in the Zeppelin NT makes a safe landing possible.

On a rigid airship the solar cells field could be affix on the envelope framework. On a blimp or a semi-rigid airship, the solar cells could be installed on the envelope as a film.



Figure 2: The 'Hindenburg' rigid airship.



Figure 3: The zeppelin NT semi-rigid airship.

6 The airship buoyancy

Aerostatic buoyancy could be determined with the help of the Archimedes' principle: 'Any object, fully or partially immersed in a stationary fluid, is buoyed up by a force equal to the weight of the fluid displaced by the object'.

The formula to calculate the airships lift force F_{lift} is described in equation 13, where V is the total Volume of the airship, g is the acceleration of gravity and $\rho(h)$ is the air density depending on the altitude.

$$F_{lift} = \rho(h) g V \quad (13)$$

Additionally required is the gravity force F_{grav} which is

$$F_{grav} = mg \quad (14)$$

and the mass m is composed of the lifting gas and the additional mass. The additional mass m_{rest} sums up the masses of all the remaining parts like the envelope, the gondola, the fins and the engines. The calculation of the airships mass is depicted in equation 15.

$$m = m_{gas} + m_{rest} = \rho_{gas} V_{gas} + m_{rest} \quad (15)$$

Moreover the airships buoyancy yields to equation 16

$$\Delta F = F_{lift} - F_{grav} = [\rho_{air} V - \rho_{gas} V_{gas} - m_{rest}] g(h) \quad (16)$$

Under the condition that $\Delta F = 0$ and dissolving this for m_{rest} (compare equation 18) the

desired maximum additional mass of the airship is

$$m_{rest} = \rho_{air}V - \rho_{gas}V_{gas} . \quad (17)$$

When the airship reaches maximum altitude the ballonets are empty to ensure a constant pressure inside the envelope. Additionally the density of air respectively helium is minimal. The minimal density on maximum altitude is indicated with the coefficient ρ_{min} . With empty ballonets the gas volume is equal to the total volume, so the additional mass on maximum altitude is the following

$$m_{rest,max} = [\rho_{air,min} - \rho_{gas,min}] V \quad (18)$$

The density of air and Helium is depending on the altitude. It can be assumed, that the Helium and the surrounding air have the same temperature and pressure. Under this conditions the density of air and Helium change uniformly by altitude.

The density ratio σ from sea level to the density on maximum altitude is given by equation 19. The same ratio holds for Helium [21].

$$\sigma = \frac{\rho_{air,min}}{\rho_{air}} = \frac{\rho_{gas,min}}{\rho_{gas}} \quad (19)$$

Using the ratio σ in equation 18 gets equation 20.

$$m_{rest,max} = \left[\rho_{air,min} - \frac{\rho_{air,min} \rho_{gas}}{\rho_{air}} \right] V = \left[1 - \frac{\rho_{gas}}{\rho_{air}} \right] \rho_{air,min} V \quad (20)$$

Finally the mass in equation 20 only depends on the air density $\rho_{air,min}$.

7 The center of mass

The center of mass (CoM) of the airship has to be below the geometric center of the airship's envelop. Only under this condition a stable flight is possible.

The general formula to calculate the CoM is given by equation 21 with the total mass m of the airship. For simplification the airship contents on pieces. The mass m_i and the distance x_i from ground while parking from the part elements have to be known.

$$CoM = \frac{1}{m} \sum_i m_i x_i \quad (21)$$

From special interest is the CoM of the solar cell field and how the CoM displaces when a solar cell field is installed. The calculation of the CoM of the solar cell field will be

introduced below.

8 Sun radiation at the airship

8.1 The different kinds of sunlight

It is necessary for the simulation to calculate the sun radiation on the airship. First of all, it is necessary to distinguish between different kinds of radiation. The largest proportion is the direct sunlight. By which are meant, as the name indicates, the rays traveled directly from the sun without interference or reflecting on obstacles or molecules.

The second part of the sunlight is the diffuse radiation. The rays are composed of former direct radiation which was scattered by molecules or suspensoids in the atmosphere [5]. Finally the ground reflected radiation. It matters near the ground so it only will take into account on flights near sea level. For flights at higher altitude reflected radiation can be neglected.

8.2 Solar constant

In literature often the solar constant G_{sc} is listed as approximately $1367[\frac{W}{m^2}]$ [5]. Strictly speaking the constant varies during the year by depending on the day of the year. The calculation regulations are shown in equation 22 where n is the n th day of the year.

$$G_{on} = G_{sc} \cdot \left[1 + 0.033 \cdot \frac{360 \cdot n}{365} \right] \quad (22)$$

The visualisation of the solar constant is shown in Figure 5 with the month of a year on the abscissa and the energy per square meter on the ordinate.

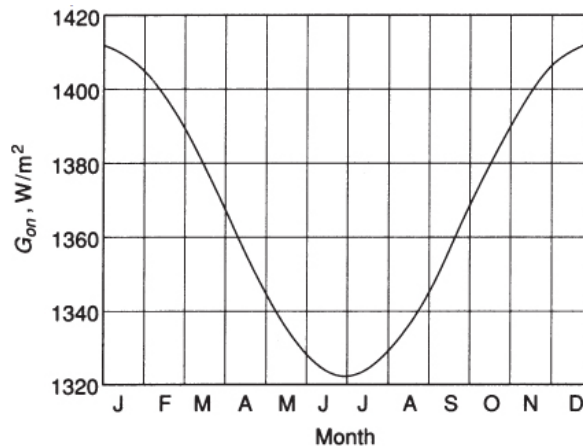


Figure 4: Variation of extraterrestrial solar radiation as a function of time of year [5].

8.3 Solar Time

For the calculation of the radiation few functions have to be defined. The first is the solar time. It is derived on the apparent angular motion of the sun across the sky [5]. The solar time t_{solar} can be calculated from the standard time $t_{standard}$. The standard time is a variable in the simulation, which gets an update after every time iteration step and therefore stores the current time. The formula for the calculation of the solar time is depict in equation 23. It applies that L_{loc} is the longitude of the location in question and $L_{standard}$ is the standard meridian for the local time zone.

$$t_{solar} = 4 \cdot (L_{loc} - L_{standard}) + E + t_{standard} \quad (23)$$

The parameter E is the *Equation of time* and the formula is shown in equation 24 where parameter B is included with the formula depict in equation 25.

$$E = 229.2 \cdot (0.000075 + 0.001868 \cdot \cos(B) - 0.032077 \cdot \sin(B) - 0.014615 \cdot \cos(2 \cdot B) - 0.04089 \cdot \sin(2 \cdot B)) \quad (24)$$

$$B = (n - 1) \frac{360}{365} \quad (25)$$

The corresponding plot to the *Equation of time* is shown in Figure 5 with the month of the year on the abscissa and the variation of the *Equation of time* in minutes on the ordinate.

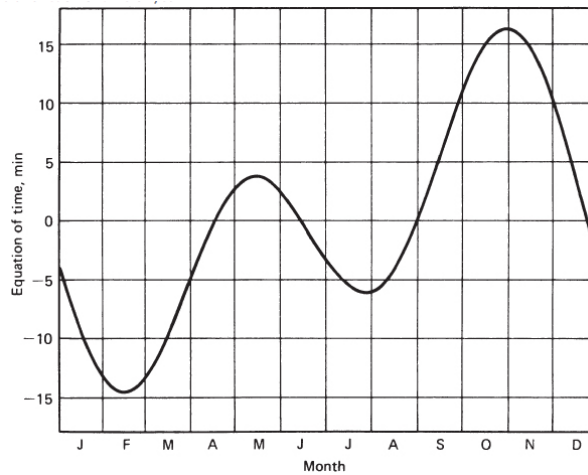


Figure 5: The equation of time E in minutes as a function of time of year [5].

8.4 Solar altitude

To understand the calculation of the direct radiation, first the air mass has to be defined. The sun's rays arrive at the beginning of the earth's atmosphere with approximately $1367[\frac{W}{m^2}]$ (for the exact value, consider equation 22).

By passing through the atmosphere the energy of the direct radiations tone down by absorbing and scattering. The value of the energy depends on how long the rays already run through the atmosphere and then depends on the angle of the sun to the ground respectively the airship.

Equation 26 describes the air mass by a given solar altitude A .

The solar mass value of $m = 1$ represents an angle of 90° which stands for the sun in zenith, so the rays have the shortest way through the atmosphere and the attenuation gets minimal [8].

$$m = \frac{1}{\sin(A)} \quad (26)$$

The solar altitude (in degrees) from equation 26 depends on the Latitude L of the current position, the declination N and the hour angle H . The calculation regulations are listed in equation 27 and all parameters are given in degrees.

$$\sin(A) = \cos(N)\cos(H)\cos(L) + \sin(N)\sin(L) \quad (27)$$

For the calculation of the hour angle the time t after solar noon is required. The hour angle H (in degree) is the angular displacement of the sun in east or west direction from the local meridian [5]. The value amounts 15° per hour (compare equation 28). The value t is the difference of the current time in solar time to solar noon which is exactly 12:00 pm. H has negative values in the morning and positive in the afternoon.

$$H = 15^\circ \cdot t \quad (28)$$

The declination N shown in equation 29, represents the seasonal variation of the position of the sun [8]. The values varies between $+23.5^\circ$ and -23.5° . The calculation of the declination requires the day of the year d after the Spring Equinox. The values for d are shown in table 2.

$$N = 23.5 \cdot \sin\left(\frac{2\pi d}{365}\right) \quad (29)$$

Table 2: Day of the year after the spring equinox.

Month	d for the i th day of the month
January	$284 + i$
February	$315 + i$
Before the 21th of march	$343 + i$
On and after the 21th of march	i
April	$10 + i$
May	$40 + i$
June	$71 + i$
July	$101 + i$
August	$132 + i$
September	$163 + i$
October	$193 + i$
November	$224 + i$
December	$254 + i$

8.5 Direct clear-sky radiation

With the solar altitude value from equation 27, an atmospheric transmittance factor τ_b of equation 30 can be calculated.

$$\tau_b = a_0 + a_1 \exp\left(\frac{-k}{\sin(A)}\right) \quad (30)$$

The formulas for the values of a_0 , a_1 and k are shown in the equations 31 to 33 and these in turn further guide to equations 34 to 36 in which the altitude h of the airship in kilometer is required. The formulas are valid for altitude less than 2.5 kilometer [16].

$$a_0 = r_0 \cdot a_0^* \quad (31)$$

$$a_1 = r_1 \cdot a_1^* \quad (32)$$

$$k = r_k \cdot k^* \quad (33)$$

The constants r_0 , r_1 and r_k are correction factors. They are listed in table 3 for different climate types.

$$a_0^* = 0.4237 - 0.00821 * (6 - h)^2 \quad (34)$$

$$a_1^* = 0.5055 - 0.00595 * (6.5 - h)^2 \quad (35)$$

$$k^* = 0.2711 - 0.01858 * (2.5 - h)^2 \quad (36)$$

Finally with the atmospheric transmittance factor τ_b the energy per square meter of the direct sunlight on a arbitrary altitude can be calculated with equation 37 using equation 30 and 22. Technically this is the energy per square meter through a plane with a normal

pointing directly on the sun.

$$P_{direct} = \tau_b \cdot G_{on} \quad (37)$$

For further purpose equation 38 specify the direct solar radiation per square meter passing through a horizontal rectangle with the size of 1 square meter.

$$\bar{P}_{direct} = P_{direct} \cdot \sin(A) \quad (38)$$

Table 3: Correction factors for climate types [16].

Climate Type	r_0	r_1	r_k
Tropical	0.95	0.98	1.02
Midlatitude summer	0.97	0.99	1.02
Subartic summer	0.99	0.99	1.01
Midlatitude winter	1.03	1.01	1.00

Clear-sky radiation for high altitude

It would also be of interest the radiation of higher altitudes. The benefit for an airship traveling on high altitudes would be a lower air density and an increase of the direct sunlight power. [8] shows an equation to calculate the direct sunlight passing through a square meter with a normal pointing to the sun depending on time and place. The formula is depicted in the following with the constant $a = 0.14$. It is valid for the whole atmosphere so altitudes up to 30 kilometers can be utilize.

$$P_{direct} = G_{on} \left[1 - \frac{a h}{1000} \right] e^{\Upsilon} + G_{on} a h \quad (39)$$

The parameter Υ is depicted in equation 40. The values for the empirical constants are $c = 0.357$ and $s = 0.678$ [8].

$$\Upsilon = -c \left[\frac{1}{\sin(A)} \right]^s \quad (40)$$

To calculate the direct radiation of a horizontal plane of 1 square meter the result P_{direct} from equation 39 has to be inserted into equation 38.

The corresponding power for altitude up to 6 km is plotted in Figure 6a, where the red graph results from the calculation using equation 38 and the blue graph from equation 39.

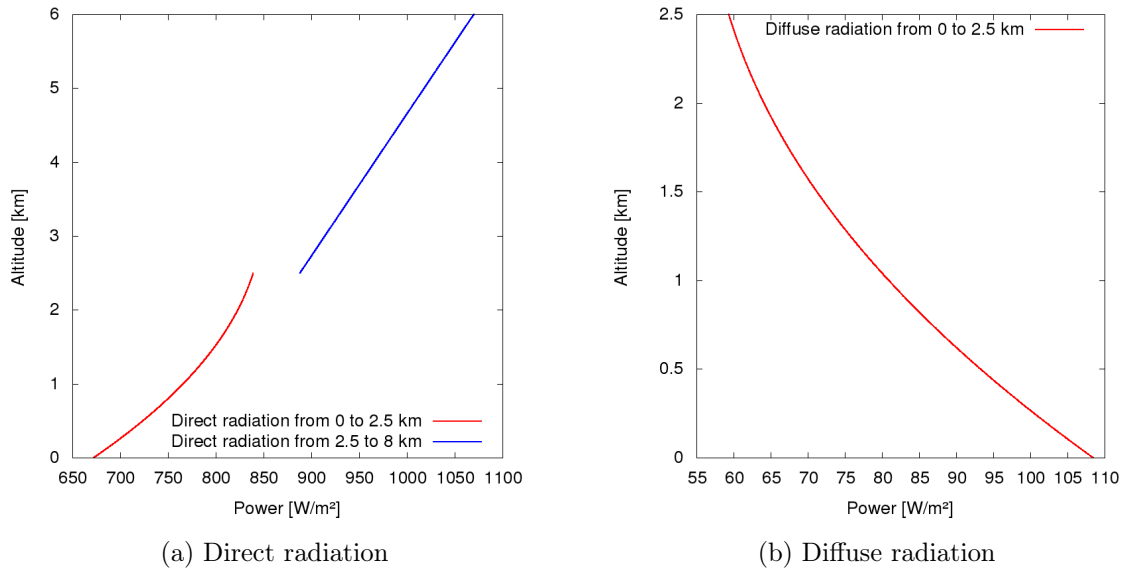


Figure 6: The power of the sun radiation depending on altitude.

8.6 Diffuse clear-sky radiation

For the simulation it is also needed to declare the diffuse radiation. For days with a clear atmosphere the radiation on horizontal plane is shown in 41 and the calculation of τ_d is based on the transmittance factor τ_b from equation 30 (compare equation 42) [17].

$$\bar{P}_{diffuse} = \tau_d \cdot G_{on} \cdot \sin(A) \quad (41)$$

$$\tau_d = 0.271 - 0.294 \cdot \tau_b \quad (42)$$

The calculation of $\bar{P}_{diffuse}$ is valid under the condition of altitude less than 2.5 kilometer. For higher altitude the diffuse radiation has to be neglected. For the corresponding power values of the sun's diffuse radiation compare Figure 6a. The power range is from almost 110 Watt on the ground to approx 60 Watt at an altitude of 2.5 kilometer. It can be noted, that on the contrary to the direct radiation the diffuse radiation decreases with rising altitude. For lower altitude the distance the rays traveled through the atmosphere is longer. This results in more interactions with particles from the atmosphere therefore more of the direct radiation is converted into diffuse radiation.

8.7 Ground reflected radiation

It can be useful to use solar cells on the bottom half of the airship to take advantage of the rays which are reflected by the ground. The effect weakens with rising altitude so the reflected radiation from equation 43 will only be considered if the airship flies near sea

level ¹ [14].

$$P_{reflected} = (\bar{P}_{direct} + \bar{P}_{diffuse}) \varrho_{ground} \frac{1 - \cos(\phi)}{2} \quad (43)$$

Angle ϕ is the slope of the solar cell where 0° is horizontal and 90° is vertical.

The factor ϱ_{ground} , is the Albedo constant which indicates the reflectance of different soil types. Therefore its value is between 1 and 0. Examples of different ground types are listed in table 4.

In a simulation which results will be presented in chapter 16 the airship travel near ground on a route in Germany. Therefore the albedo value will be set to the mean value of forrest ², which is 0.125 (compare Table 4).

Table 4: Albedo values for certain surfaces [15] [14].

Surface	Albedo
Absolute black surface	0
Calm sea surface	0.02 - 0.04
Forrest	0.05 - 0.2
Green grass	0.08 - 0.27
Sand	0.2 - 0.4
Snow	0.75 - 0.85
Absolute white surface	1

9 The discretization of the airship

9.1 The geometry as an ellipsoid

In this simulation the shape of the airship is an ellipsoid with a defined length and diameter. The simulation also differs between solar cells only on the top half of the airship and an airship fully covered in solar cells. The reason to have solar cells on the top half is to catch the direct sunlight. Diffuse radiation can equally be caught on the whole airship surface. It may be an advantage to cover the whole surface in solar cells even though the disadvantage of the gaining weight and the higher budget of the additional cells.

If the airship travels ground near, the rays reflected from the ground have to take into account. Using the energy of these rays is only possible with solar cells on the bottom half of the airship.

The ellipsoid is parameterized with the angles θ and ϕ .

An arbitrarily point (x, y, z) on the surface can be calculated by equation 44, 45 and 46.

$$x = a \cdot \cos(\theta) \cos(\phi) \quad (44)$$

¹Less than 150 meter of altitude

²Forrest covers most of the ground in Germany [33].

$$y = b \cdot \cos(\theta) \cos(\phi) \quad (45)$$

$$z = c \cdot \cos(\theta) \sin(\phi) \quad (46)$$

The angle θ has the range shown in equation 47 and ϕ has the range shown in 48. The range of ϕ depends on whether it is a full ellipsoid or only the upper half.

$$-\pi \leq \theta \leq \pi \quad (47)$$

$$\phi \in \begin{cases} [0, \frac{\pi}{2}], & \text{for the upper half of the ellipsoid} \\ [0, \pi], & \text{for the whole ellipsoid} \end{cases} \quad (48)$$

For the simulation it is necessary to calculate the angle between the direct radiation of the sun and the solar cells. Therefore the surface of the airship is divided into small rectangle parts.

Algorithm 1 shows the calculation of the surface parts. Line 1 and 2 implement the nested loop which was described in equation 47 and 48. In this case the nested loop is iterating over the whole upper half of the ellipsoid. The current position on the surface of the airship is point (x_1, y_1, z_1) (compare the calculation in Algorithm 1 line 3 - 5). Point (x_2, y_2, z_2) is beside that point (x_1, y_1, z_1) because θ is 1 step h ahead.

Nearly the same holds for (x_3, y_3, z_3) . In this case ϕ is 1 step h ahead, so the point is below the current point (x_1, y_1, z_1) .

Line 12 calculates the distance of (x_1, y_1, z_1) and (x_2, y_2, z_2) and line 13 the distance of (x_1, y_1, z_1) and (x_3, y_3, z_3) . Furthermore s and h determine the rectangle A from the three described points on the surface (compare line 14).

Therefore in every iteration step a small part of the hull with given size is taken into account. All steps together and thus all area parts depict the complete upper half of the envelope. In addition the angle θ and ϕ are known.

The same holds for a solar cell field covering all of the envelope.

With this information, below in this thesis, the amount of power the solar cell field on the airships hull generates can be determined.

In the simulation the discretisation of the surface is also used to calculate the center of mass of the solar cell field. The distance from the ground can be determined in every iteration step with the help of equations 44 to 46. The CoM is the average of of these heights because the evaluation points while iterating are equally distributed on the ellipsoids surface.

Algorithm 1 Calculation of the rectangular surface parts of the upper half of the airship

```

1: for  $\theta \in \{-\pi, \dots, \pi\}$  do
2:   for  $\phi \in \{0, \dots, \pi/2\}$  do
3:      $x_1 = x \cdot \cos(\theta) \cdot \sin(\phi)$ 
4:      $y_1 = x \cdot \sin(\theta) \cdot \sin(\phi)$ 
5:      $z_1 = x \cdot \cos(\phi)$ 
6:      $x_2 = x \cdot \cos(\theta + h) \cdot \sin(\phi)$ 
7:      $y_2 = x \cdot \sin(\theta + h) \cdot \sin(\phi)$ 
8:      $z_2 = x \cdot \cos(\phi)$ 
9:      $x_3 = x \cdot \cos(\theta) \cdot \sin(\phi + h)$ 
10:     $y_3 = x \cdot \sin(\theta) \cdot \sin(\phi + h)$ 
11:     $z_3 = x \cdot \cos(\phi + h)$ 
12:     $s = \sqrt{(x_1 - x_2)^2 + (y_1 - y_2)^2 + (z_1 - z_2)^2}$ 
13:     $h = \sqrt{(x_1 - x_3)^2 + (y_1 - y_3)^2 + (z_1 - z_3)^2}$ 
14:     $A = s \cdot h$ 
15:   end for
16: end for

```

9.2 The solar azimuth angle

For further calculations the angular displacement Z is necessary. It is the direction displacement of the sun's geographic north with negative angles for a displacement to the east direction and positiv angle for displacement to the west direction. An illustration of the azimuth angle is shown in Figure 7 and the corresponding equation is displayed in equation 49. For the calculation the solar altitude, the hour angle and the declination are required (the formulas can be found in equation 27 to 29)

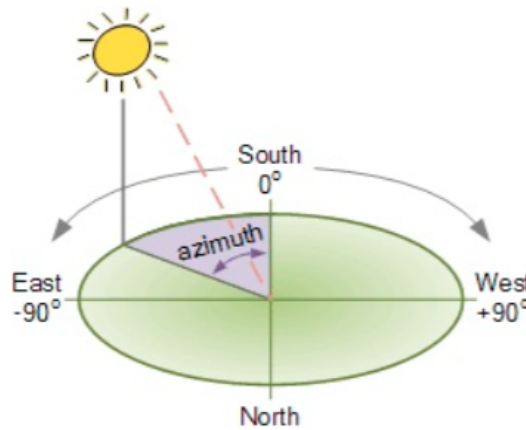


Figure 7: The sun azimuth angle [18].

$$Z = \sin^{-1} \left(\frac{\cos(N)\sin(H)}{\cos(A)} \right) \quad (49)$$

9.3 The power generation of the airship surface

So far the airship hull was splitted into arbitrary small rectangular parts (compare Algorithm 1). The next step is the calculation of the energy production of every rectangular part of the surface. Equation 50 calculates the solid angle of the normal of the surface part and a vector pointing directly at the sun [19]. A is again the solar altitude angle and Z the solar azimuth angle. The angles θ and ϕ are the loop variables from line 1 and 2 of the algorithm while $\bar{\phi}$ was amend by the formula in equation 51.

$$B = \cos^{-1} (\cos(A) \cdot \cos(Z - \theta) \cdot \sin(\bar{\phi}) + \sin(A) \cdot \cos(\bar{\phi})) \quad (50)$$

$$\bar{\phi} = 90^\circ - \phi \quad (51)$$

Of course solid angles of more then 90° do have to be neglected, because in this case non of the rays would reach the solar cell (compare equation 52). This cell would be on the shadow side of the airship. For solid angles B between 0° and 90° the proportion factor $\eta_{i,direct}$ of the power from \bar{P}_{direct} can be calculated with equation 52

$$\eta_{i,direct} = \begin{cases} 0, & \text{else} \\ \cos(B), & 0^\circ < B < 90^\circ \end{cases} \quad (52)$$

Equation 41 shows the calculation of the diffuse radiation on a horizontal plane respectively a horizontal solar cells. To convert for tilted solar cells, [11] suggests a linear decrease in the range from 1.0 (horizontal solar cells) to 0.5 (vertical solar cells). The proportion factor $\eta_{i,diffuse}$ of the power from $\bar{P}_{diffuse}$ is given by equation 53.

$$\eta_{i,diffuse} = \frac{\phi}{\pi} + 0.5 \quad (53)$$

The total value of the produced energy under the condition of direct radiation is given by equation 54. The equation sums up over all surface parts with area A (compare Algorithm 1), the proportion factor $\eta_{i,direct}$ and the energy of the direct solar radiation \bar{P}_{direct} .

Moreover the efficiency of a solar cell η_{solar} comes into play. A solar cell cannot convert all the energy of the rays into electrical power. State of the art solar cells are capable of efficiency factors of circa 25 % which was used for η_{solar} in the following simulations [34].

$$P_{direct,total} = \sum_i [\eta_{i,direct} \cdot \bar{P}_{direct} \cdot \eta_{solar} \cdot A] \quad (54)$$

Same holds for the total produced energy from diffuse radiation. It is shown in equation 55.

$$P_{diffuse,total} = \sum_i [\eta_{i,diffuse} \cdot \bar{P}_{diffuse} \cdot \eta_{solar} \cdot A] \quad (55)$$

The total generated power the solar cell field produces is the sum of the diffuse and direct rays power. It is shown in the following equation.

$$P_{total} = P_{direct,total} \cdot P_{diffuse,total} \quad (56)$$

10 The Engine of the airship

The goal of this chapter is to calculate the airships thrust from equation 2. The general relation is depict in equation 57. P_{use} is the effective power after deduction of losses, which can be used to speed up the airship [23].

$$F_{thrust} = \frac{P_{use}}{v} \quad (57)$$

It is striking in equation 57, that if the velocity is 0 there is no thrust although power supply holds. For this steady state, reference [24] provides equation 58.

$$F_{thrust} = \sqrt[3]{2\rho A_s P^2} \quad (58)$$

Using equation 57 for the calculation of thrust during the flight with $v \neq 0$, the thrust can also be calculated by the power P_{prop} which is the power that runs directly into the propellor and the velocity v_s which is the velocity directly at the propellor (compare equation 59 and Figure 8) [23].

$$F_s = \frac{P_{prop}}{v_s} \quad (59)$$

The theoretical efficiency η_{th} is the ratio of the effective power P_{use} and the power at the propellor P_{prop} (compare equation 60). η_{th} represents the factor of energy which gets lost by transforming the energy produced by the solar cell field, to generate the thrust with the help of the engine.

$$\eta_{th} = \frac{P_{use}}{P_{prop}} = \frac{v * F_s}{v_s * F_s} = \frac{v}{v_s} \quad (60)$$

Source [24] presents some other relations.

The area of a propellor A_{prop} can be calculated with the diameter d_{prop} (compare equation 61).

$$A_{prop} = \frac{d_{prop}^2 \pi}{4} \quad (61)$$

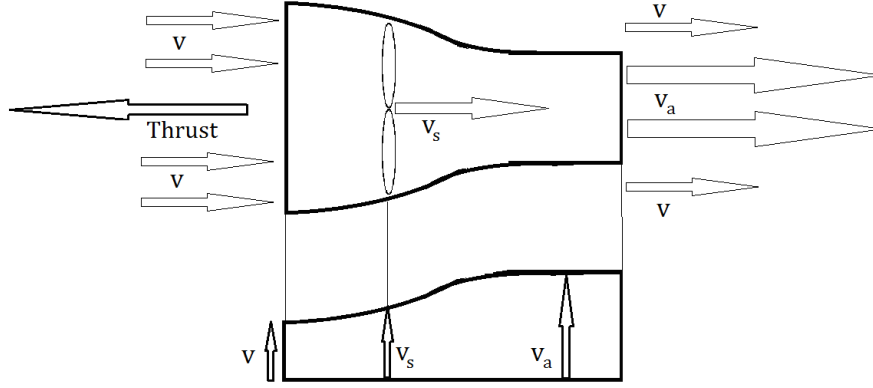


Figure 8: Cross-section of a propellor engine and the corresponding velocities.

In Figure 8 there are three different velocities drawn and equation 62 shows the corresponding equation. The velocity v is the velocity the airship is traveling with, therefore which is entering the propellor engine. The velocity v_a is the velocity of the air escaping the engine at the end. The value of v_a is higher than v because of the air acceleration caused by the propeller movement. This can be seen in the visualisation of the velocity in the lower half of Figure 8. Propeller engines are normally built such that half of the acceleration is because of the pulling in of the air and the second half is the air pulling off. This means that the velocity v_s at the propeller must be in the mean value of v and v_a (compare equation 62).

$$v_s = \frac{v + v_a}{2} \quad (62)$$

The thrust F_{thrust} the propellor creates can be calculated by the volume flow \dot{V} and the change of the air's velocity. The formula is shown in equation 63.

$$F_{thrust} = \rho \dot{V} (v_a - v) \quad (63)$$

The volume flow is defined as an area the flow is crossing times the velocity. The reference point of the volume flow is the propellor in the engine so the reference area is the area of the propellor and the reference velocity is the air's velocity at the propellor. The equation is depicted in the following.

$$\dot{V} = v_s A_{prop} = \frac{v + v_a}{2} A_{prop} \quad (64)$$

Dissolving equation 64 for v_a gets to equation 65.

$$v_a = \frac{2\dot{V}}{A_{prop}} - v \quad (65)$$

The resulting equation is now to be inserted into the thrust calculation (equation 63) and leads to equation 66, which brings the desired quadratic function

$$F_{thrust} = \rho \dot{V} \left(\left(\frac{2\dot{V}}{A_{prop}} - v \right) - v \right) = \frac{2\rho \dot{V}^2}{A_{prop}} - 2\dot{V}v\rho \quad (66)$$

This quadratic function can be solved for \dot{V} except for the unknown thrust F_{thrust} . Equation 67 has 2 solutions. The first solution is positive and the second solution is negative. Only a positive solution for the volume flow is reasonable, so the negative solution will be ignored.

$$0 = \frac{2\rho \dot{V}^2}{A_s} - 2\dot{V}v\rho - F_{thrust} \quad (67)$$

Assuming the thrust F_{thrust} is known, the velocity v_a at the end of the engine can be calculated by additional help of the volume flow \dot{V} , the air density ρ and the velocity of the airship v . This can be done with equation 63 dissolving for v_a in equation 68.

$$v_a = \frac{F_{thrust}}{\rho \dot{V}} + v \quad (68)$$

Using equation 60 and 62 η_{th} can be calculated with the air velocity entering and leaving the propellor engine (compare equation 69).

$$\eta_{th} = \frac{2}{1 + \frac{v_a}{v}} \quad (69)$$

With the known efficiency η_{th} , the provided power to the propellor P_{prop} and the velocity of the airship v the thrust F_{thrust} can be determined, as in equation 70.

$$F_{thrust} = \frac{P_{use}}{v} = \frac{\eta_{th} P_{prop}}{v} \quad (70)$$

The challenge is that the end result of equation 70 is the thrust F_{thrust} , but the same thrust is needed to calculate the result (compare equation 66). The solution for this issue is to calculate the final thrust value as the result of a loop. The first iteration step is by using an arbitrary thrust in equation 66³. With this guess a new thrust value will be calculated. By inserting it back into equation 66 again and calculate the new thrust and repeating this more often the thrust and the efficiency will approach their real values.

The real efficiency is even lower. In addition η_{prop} which stands for the losses of friction has to be considered. A propellor is never shaped ideal. [25] suggests a value of $\eta_{prop} = 82\%$. Furthermore an electric engine has also, an efficiency value. Nowadays they are very well

³In the simulation the thrust from the last time step will be used for faster convergence.

developed so an efficiency of 98% [35] was chosen for η_{motor} . The calculation for the total efficiency is shown in equation 71.

$$\eta = \eta_{th} \eta_{prop} \eta_{motor} \quad (71)$$

So far the algorithm assumes, that all provided energy is put into one engine. The energy P_{prop} needs to be divided by the number n_{motor} of engines ⁴. The final relation between power and thrust is depict in equation 72

$$F_{thrust,i} = \frac{P_{prop} \cdot \eta}{v \cdot n_{engine}} = \frac{P_{prop} \cdot \eta_{th} \eta_{prop} \eta_{motor}}{v \cdot n_{motor}} \quad (72)$$

Finally when the thrust of one engine is determined, the total thrust is the sum of the thrust of every engine (compare equation 73)

$$F_{thrust} = \sum_i^{n_{motor}} F_{thrust,i} \quad (73)$$

The presented algorithm is again summarized in Algorithm 2. The algorithm uses a loop to approach η_{th} and completes when the value is accurate enough (compare line 3 and 9f). It is also worth mentioning the calculation of \dot{V} in line 5, with the help of line 1f and 4. It uses the quadratic equation 66 to solve for the volume flow.

Algorithm 2 Calculation of the thrust and the theoretical efficiency of an airship.

```

1:  $a = 2\rho A_{prop}$ 
2:  $b = -2v\rho$ 
3: while true do
4:    $c = -F_{thrust}$ 
5:    $\dot{V} = \frac{(-b + \sqrt{b^2 - 4ac})}{2a}$ 
6:    $v_a = \frac{F_{thrust}}{\rho \dot{V}}$ 
7:    $\eta_{th} = \frac{2}{1 + \frac{v}{v_e}}$ 
8:    $F_{thrust} = \frac{P_{prop} \eta_{th} \eta_{prop} \eta_{motor}}{v n_{motor}}$ 
9:   if  $|\eta_{th} - \eta_{th,old}| < tol$  then
10:     break
11:   end if
12:    $\eta_{th,old} = \eta_{th}$ 
13: end while
```

⁴It is assumed that all engines get the same amount of energy.

The variation of the engines efficiency

Equation 66 points out that the theoretical efficiency of an engine depends on the air density. The plot in Figure 9a shows the relation between the altitude (on the ordinate) and the corresponding efficiency (on the abscissa). The efficiency varies from approx. 62 % near the ground to 51 % on 8 kilometer flight level. The efficiency of the engine lowers by rising altitude, because the propellor uses air with lower density to suck in and to push away.

The disadvantage of the lower efficiency is on the contrary to the advantage of the decreasing drag force by flights in higher altitude. Further simulation results will demonstrate which effect dominates.

Another impact on the efficiency has the number of engines on an airship. By increasing the number of engines, the power a single engine has to convert into thrust decreases. This effects the theoretical efficiency of each engine. The relation of the efficiency by the number of engines is shown in Figure 9b. The range of the efficiency values on the abscissa starts with approx 62 % with one engine to 87 % by using eight engines. It is visible that the effect of increasing efficiencies by increasing the number of engines weakens. For an infinite number of engines the theoretical efficiency would reach 100 %.

The remaining input data for the presented simulations are listed in the appendix A.

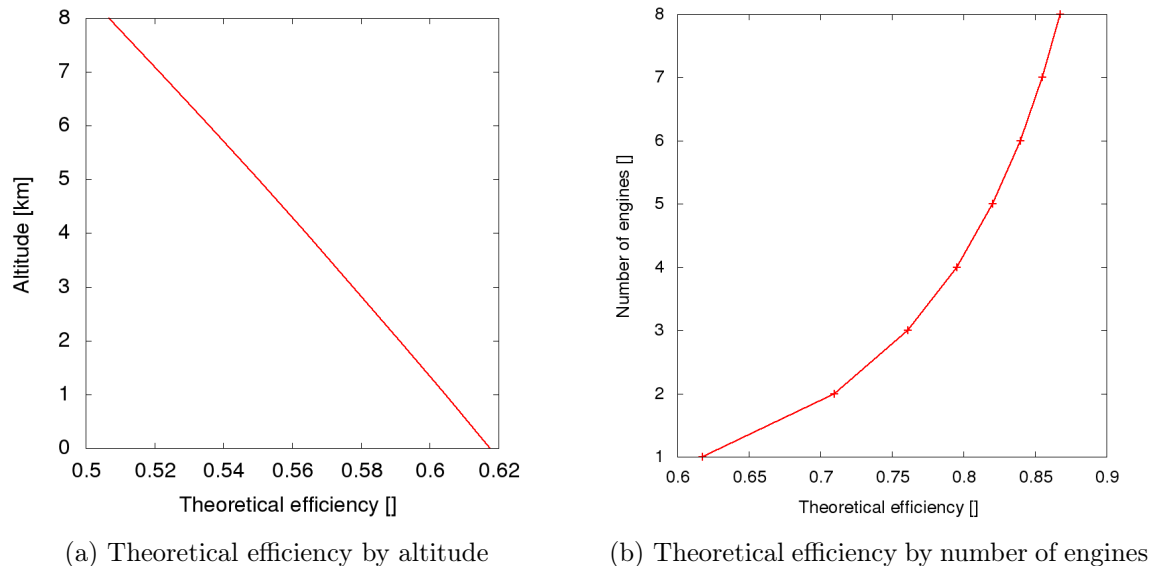


Figure 9: Variation of theoretical efficiency.

11 Geographic coordinates

Section 8 points out that latitude and the longitude are necessary to calculate the power of the sunlight which reaches the airship. The simulation starts on a certain point with

given longitude and latitude but the simulation calculates a distance in x and y in every timestep (compare equation 5).

Therefore the current longitude and latitude is needed to calculate the value of the sunlight on the current position of the airship. It appears that conversional functions are necessary to update the longitude and latitude by a given distance in x and y direction.

[7] gives an equation which is shown in equations 74 and 75, to calculate new geo coordinates by giving geo coordinates and a distance and an angle.

$$\phi_{n+1} = \arcsin(\sin \phi_n \cdot \cos \delta + \cos \phi_n \cdot \sin \delta \cdot \cos \theta) \quad (74)$$

$$\lambda_{n+1} = \lambda_n + \arctan(\sin \theta \cdot \sin \delta \cdot \cos \phi_n, \cos \delta - \sin \phi_n \cdot \sin \phi_{n+1}) \quad (75)$$

Value ϕ_n is the last latitude value and ϕ_{n+1} is the updated latitude value for the next time step. The similarity applies to λ_n and λ_{n+1} as the longitude value.

Furthermore θ is the angle of the direction with a range from 180° to 180° , clockwise from north [7]. The value δ is the angular distance which is calculated as shown in equation 76.

$$\delta = \frac{d}{r} \quad (76)$$

Value d is the distance, in kilometer which the airship flew in the timestep and the earth radius is defined as r in kilometer ⁵. The general distance, the airship traveled in x and y direction in one timestep can be calculated by equation 77

$$d = \arctan\left(\frac{\Delta y}{\Delta x}\right) \quad (77)$$

The longitude and latitude values from equation 74 and 75 are required in radians not in degrees, in difference to the other calculations in the simulation. So in the beginning of the geo coordinate calculation the coordinates have to be converted to radians and afterwards back to degrees.

12 Weather data

There is a way to get results closer to the reality. It is by using real weather data. The german weather service called 'Deutscher Wetter Dienst' provides all kinds of weather data on a public server.

There are data files available for Europe in total but especially for Germany. This server files weather data for different time periods. There are seasonal period, monthly daily and even hourly data records. On special interest for the simulation are hourly data sets

⁵For this purpose a mean value of 6.371 km for the earth radius is sufficed enough

because the weather data the simulation requires changes significantly during the day. A restriction is that the hourly records are only available for a german grid in german weather service database.

In chapter 4 equations were presented which may use some values from the weather database. In the simulation the calculation of temperature (compare equation 11) and pressure (compare equation 10) will insert values from the database for a given time and location.

Furthermore german weather service provides data for velocity and the direction of the wind. These records will take into account to simulate more realistic scenarios.

12.1 Access on the weather data

The weather data is stored on a ftp-server in the NetCDF format [26] [27]. NetCDF is a binary format developed from the Common Data Format originally created by NASA. It is not possible to access the data directly by reading in the files, but with the help of the NetCFD program-library.

The header information of the hourly weather data files for Germany is a grid stored with 720 steps in abscissa (x) direction and 938 steps in ordinate (y) direction. This is the first and second dimension. There is also a third dimension, the time stored in one file. The time dimension has 744 entries. 24 entries per day times, 30 days per month. Also in the header information is a description about the access function the library can address.

Always available are two functions that return the longitude respectively the latitude for a given x respectively y value. There is also a function provided to read one weather data value for example the temperature or the pressure. The function needs as parameter values from the three dimension, a x, a y and a time value. The parameter, in this case x and y indicates that the access function is to optimize for sequential access by x and y. For the simulation the weather data for a given longitude and latitude is needed. The approach is to first get the x and y value for the known longitude and latitude and after getting the weather data value.

The algorithm to calculate the x and y value is listed in Algorithm 3. To increase data access speed the algorithm uses a binary search to get the longitude and latitude value. The working method of this search will be explained below.

The algorithm contains a while loop (compare line 1) which iterates until termination condition is reached (compare line 16 and 18) The first step in the loop is to query the longitude and latitude value for a given x and y value (compare line 2 and 3). Therefore as an argument, the functions needs an array with 2 values where the first entry is the x value and the second is y value. For faster convergence the array is initialize with $x = \frac{nx}{2}$ and $y = \frac{ny}{2}$ where nx is the grid length in x dimension and ny is the grid length in y

dimension.

Later on the new latitude gets compared with the wanted latitude (compare line 4). If the latitude is smaller, as the wanted latitude, then the *indexLatLeft* variable is set to the current latitude index (compare line 5). If it is higher then *indexLatRight* is set to the current latitude index (compare line 7). The *indexLatLeft* and *indexLatRight* are the boundaries of an interval in which the wanted x index is included. By deciding whether the index is on the left or on the right side of the interval, it gets smaller by half of its size in every iteration step. After the reduction of the interval the new x index is set to the middle of the new interval which is seen in line 9.

The same calculation holds for the corresponding longitude index (compare line 10 to 15). The loop terminates, if the value of the x and y index didn't change in the current iteration. The desired x and y index is now stored in the *indexLatLon* array. With these values and a time value, the query function for the weather data values can be called to access, e.g. a temperature value.

Algorithm 3 Calculate the x and y value for a given latitude and longitude value

```

1: while true do
2:   lat = getLatitude(indexLatLon)
3:   lon = getLongitude(indexLatLon)
4:   if lat < searchLat then
5:     indexLatLeft = indexLatLon[0]
6:   else
7:     indexLatRight = indexLatLon[0]
8:   end if
9:   indexLatRight[1] = (indexLatLeft+indexLatRight)/2
10:  if lon < searchLon then
11:    indexLonLeft = indexLatLon[1]
12:  else
13:    indexLonRight = indexLatLon[1]
14:  end if
15:  indexLonRight[1] = (indexLonLeft+indexLonRight)/2
16:  if indexLatLon[0] == indexLatOld && indexLatLon[1] == indexLonOld then
17:    calculateWeatherDataValue()
18:    break
19:  end if
20:  indexLatOld = indexLatLon[0]
21:  indexLonOld = indexLatLon[1]
22: end while

```

12.2 Wind data

Compared with an airplane an airship has more front and side faces. This makes the airship assailable to wind. Wind blowing from the front can slow down the airship distinctly but on the other hand a back wind can rise the velocity of the airships.

The chapter before explained the access to the weather data. Wind data is stored in two files, one for the wind speed and one for the wind direction.

For this simulation only the back and the front wind will be considered because only these have a huge impact on the airship's velocity. The goal is to calculate the proportion of back or front wind from the wind data. At first the direction of the airship has to be calculated by using equation 78. The atan2 function returns the result in radiants so $\frac{180^\circ}{\pi}$ has to be added to the equation for the result in degree.

$$\bar{\alpha}_{zep} = atan2(\Delta x, \Delta y) \cdot \frac{180^\circ}{\pi} \quad (78)$$

The result of equation 78 is in a range from -180° to 180° . Equation 79 converts the result to the desired range from 0° to 360° .

$$\alpha_{zep} = \begin{cases} 360^\circ - |\bar{\alpha}_{zep}|, & \bar{\alpha}_{zep} < 0^\circ \\ \bar{\alpha}_{zep}, & \text{else} \end{cases} \quad (79)$$

The wind direction value from the weather data file returns a value from 0° to 360° , so the angle between the airship and the wind can be calculated by subtracting them. The proportion of the front respectively back wind is calculated by the cosinus of this angle which is listed in the following.

$$v_{wind} = \cos(|\alpha_{zep} - \alpha_{wind}|) \quad (80)$$

The force of the wind on an airship can be calculated in the same manner as the drag force. Equation 6 is used and instead of the velocity of the airship, the wind velocity is inserted. In the case of front wind the resulting wind force from equation 6 is multiplied by -1. That implies a negative force value for front winds and a positive for back winds. With the resulting wind force F_{wind} equation 2 can be extended to equation 81.

$$F = F_{thrust} + F_{drag} + F_{wind} \quad (81)$$

The wind data were measured 6 meter above the ground. In the simulation the airships will fly in higher altitudes. There is a possibility to approximate the wind velocity for higher air levels by the wind velocity from the ground. The wind force increases with altitude, because friction with obstacles on ground negligible. But this effect decreases by rising altitude. The wind velocity profile scales logarithmic. The corresponding function is described in equation 82. The known wind velocity v_0 which was measured at height h_0 from the ground. Value z_0 is the surface roughness which is defined in meter. In this simulation it is set to $z_0 = 0.8 \text{ m}$ for forrest terrain which is most common in Germany.

$$v_{wind} = v_0 \frac{\ln\left(\frac{h}{z_0}\right)}{\ln\left(\frac{h_0}{z_0}\right)} \quad (82)$$

This equation only holds for the surface-layer of the Planetary boundary layer so only for a few hundred meter [32].

13 Analytical formula for the airship velocity

To verify the results of the simulation an analytic equation for the velocity of the airship is presented in this section. Equation 72 from section 10 shows the calculation of the thrust. Additionally equation 6 from section 3 describes the drag force calculation. By treating them as equivalent equation 83 follows.

$$F_{thrust} = F_{drag} \quad \rightarrow \quad \frac{P \cdot \eta}{v} = \frac{1}{2} \rho v^2 A_s c_w \quad (83)$$

Transposing the equation to find v gives the 3th. square root equation 84. With this formula an analytic solution for the airship velocity can be calculated.

$$v = \sqrt[3]{\frac{2P\eta}{c_w A_s \rho}} \quad (84)$$

The same formula can also be dissolved for the efficiency. It will be used to verify the simulation results.

$$\eta = \frac{\rho v^3 A_s c_w}{2 \cdot P} \quad (85)$$

Verification of the engine efficiency

The first verification will be the theoretical efficiency η_{th} from section 10. Two airships with known technical data will be used. The airship LZ 129 better known as 'Hindenburg'. Literature gives relevant values to estimate the efficiency of the 'Hindenburg'. With the length of 245 m, a maximum diameter of 41.2 m and the envelope volume of $2.0 \cdot 10^5 m^3$ it is possible with the help of equation 7 and 8 to determine the drag coefficient and the surface area. The values are shown in Table 6 [28].

Furthermore [29] gives the information of four engines with a maximum power of 984 KW each, so the total power is 3.936 MW.

With the known maximum velocity of $135 \frac{km}{h}$ equation 84 can be transposed to find the total efficiency η . With a known total efficiency η and equation 71 the theoretical efficiency η_{th} can be determined.

In this case $\eta_{motor} = 100\%$ because in the energy power value of 984 KW the efficiency of the motor is already taken into account.

The second airship for comparison is the Zeppelin NT. Three engines with 149 KW, each effect a maximum velocity of $125 \frac{km}{h}$. The airship has three engines. Two are equipped with a propellor with 2.5 m diameter and one with 2.2m. For this purpose it is sufficient enough to use the mean value of the three propellor diameter [31].

The number of engines n_{motor} has to be set to one as an input parameter for Algorithm

2. The reason is that the analytic formula from equation 85 does not take the number of engines the airship uses into account. Which means the efficiency from the analytic formula can be compared with the solution of the algorithm by setting $n_{motor} = 1$. The additional input parameter for equation 84 and Algorithm 2 are also listed in Table 6.

For the 'Hindenburg' the calculated theoretical efficiency η_{th} with the help of the analytical formula of equation 85 is 79.78 %. Furthermore for the Zeppelin NT, the result of η_{th} is 67.14 %.

The calculated theoretical efficiency to compare from Algorithm 2 is 69.87 % for the 'Hindenburg' and 72.69 % for the Zeppelin NT airship.

The results are listed in Table 5. There is also listed the total efficiency of the airships and the error of the analytical and the simulation result.

There are only assumptions possible about the reason of the error. Certain simplifications had to be made in this thesis. For example the calculation of the drag coefficient and the surface area assume an elliptical shape. This is only correct in good approximation. In actual fact, the shape of the envelope is more like a fluid drop. Also an effect on these values have the fins the engines and the gondula although they are small in compare to the hull.

For an exact estimation of the drag coefficient and the surface area, a model of the airship should be build. With the model inside a wind tunnel the experimental value for these values can be approximated. But this would lead beyond this theoretical thesis.

Futhermore the used value for the efficiency of the propellor is only a general reasonable value. It is not the exact value for one of the calculated airships and it comes in addition, that at the beginnning of the 19th century when the 'Hindenburg' was build the construction opportunities were not as advanced as today. The propellor efficiency may differ.

Table 5: The efficnsy of the 'Hindenburg' and the Zeppelin NT.

	'Hindenburg'	'Zepelin NT'
Analytical: η_{th}	79.78%	67.14%
Simulation: η_{th}	69.87%	72.69%
Analytical: η	65.42%	55.05%
Simulation: η	57.69%	59.61%
Error	12.42%	8.27%

Table 6: Specification of the 'Hindenburg' and the Zeppelin NT airship.

	'Hindenburg'	'Zeppelin NT'
Power: P	$3.936 \cdot 10^6 W$	$4.47 \cdot 10^5 W$
Velocity: v	$135 \frac{km}{h}$	$125 \frac{km}{h}$
Density: ρ	$1.225 \frac{kg}{m^3}$	
Drag coefficient: c_w	0.0233	0.0235
Surface area: A_s	$3419.95 m^2$	$408.46 m^2$
Propellor efficiency: η_{prop}	82%	
Motor efficiency: η_{motor}	100%	
Propellor diameter: d_{prop}	6m	2.53m
Number of engines: n_{motor}	4	3

14 Value settings of the simulated airships

Two different airships will be observed. They were already introduced. The first is an airship with the dimensions of the LZ-129 better known as 'Hindenburg'.

The second airship is a smaller semi rigid airship based on the Zeppelin NT. The Zeppelin NT is a state of the art airship which is currently being manufactured.

The simulation input parameter for the two airships are listed in Table 7.

Table 7: Input parameter for the simulated flights.

	'Hindenburg'	Zeppelin NT
Max. altitude: h_{max}	6km	
Envelope volume: V	$2.0 \cdot 10^5 m^3$	$8255 m^3$
Max. diameter: d	41.2 m	14.16
Length: l	245 m	75 m
Drag coefficient: c_w	0.0233	0.0235
Surface area: A_s	$3419.95 m^2$	$408.46 m^2$
Reynolds number: Re	$1.138 \cdot 10^7$	$1.00 \cdot 10^7$
Num. of engines: n_{motor}	4	3
Solar cell efficiency: $\eta_{solarcell}$	25%	
Solar cell mass density: ρ	$0.42 \frac{kg}{m^2}$	
Propellor efficiency: η_{prop}	82%	
Propellor diameter: d_{prop}	6 m	2.53 m

15 Requirement checks

15.1 The buoyancy and maximum altitude of the airships

The buoyancy and the mass of the airship strongly depends on the targeted maximum flight height. For the airship mass calculation equation 20 has to be considered to deter-

mine the maximum altitude. The resulting masses for the 'Hindenburg' and the Zeppelin NT are depict in Figure 10. The ordinate shows altitude in the range of 0 to 8 km with a stepsize of 1 km. The abscissa is divided. The bottom abscissa shows the remaining mass of the Hindenburg in tons and the upper abscissa the mass of the Zeppelin NT in tons. The range for the 'Hindenburg' is from approx. 210 tons for ground near flights only to approx. 90 tons for flights with a maximum altitude of 8 km. The remaining mass for the Zeppelin NT is approx. 8.7 tons for ground near flights and approx. 3.7 tons for flights level up to 8 km. The values for all maximum altitude can be found in the appendix section B in Table 15.

In this simulation the ambition is to travel up to 6 km of altitude, where the air density amounts $\rho(6\text{ km}) = 0.660 \frac{\text{kg}}{\text{m}^3}$. Four different configurations will be demonstrated, the 'Hindenburg' and the Zeppelin NT airship each provided with a solar cell field but only on the top half of the envelope and with a solar cell field all over the envelope.

The solar cell field of the 'Hindenburg' weights 5.3 t for only the top half of the envelope and 10.6 t if the bottom half is covered as well. The mass for the remaining parts of the 'Hindenburg' is 108.3 t , respectively 103.0 t , depending on the size of the solar field.

The mass of the solar field is 560 kg for the top half and 1.1 t if the top and the bottom half is covered with solar cells. Therefore the remaining mass yields 4.1 t for the first configuration and 3.6 t for the second configuraton. The masses of the different configurations are listed in table 8 and 9.

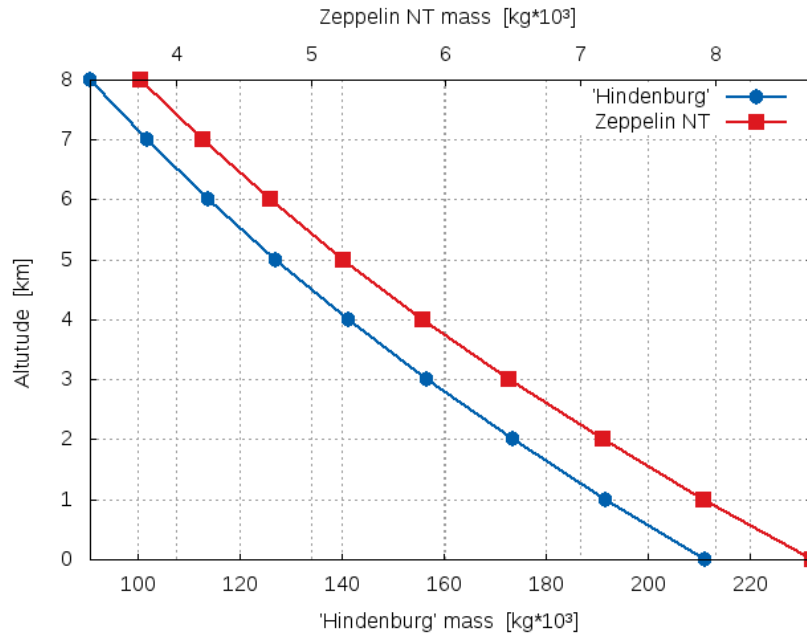


Figure 10: The airships mass by maximal altitude.

Table 8: Parameter for an airship with solar cells on the top half of the hull.

	'Hindenburg' [$kg \cdot 10^3$]	Zeppelin NT [$kg \cdot 10^3$]
Total mass:	113.6	4.7
Solar cell field mass:	5.3	0.56
Remaining mass:	108.3	4.2

Table 9: Parameter for an airship with the hull totally covered in solar cells.

-	'Hindenburg' [$kg \cdot 10^3$]	Zeppelin NT [$kg \cdot 10^3$]
Total mass:	113.6	4.7
Solar cell field mass:	10.6	1.1
Remaining mass:	103.0	3.6

The dependency of the airships mass on the velocity

In this paragraph the dependency of the airships mass on its velocity is to be investigated. Equation 3 shows the relation between mass and acceleration, so the mass is not directly connected with the calculation of the velocity.

Figure 11 depicts the velocity on the ordinate of the 'Hindenburg' with different masses. The mass range is from 50 to 200 tons. On the abscissa the time is plotted and on the ordinate the velocity. The flight starts at 11:00 pm and approximately the first 5 min is displayed.

All simulated flights are reaching the same velocity only with different fast convergence. The more the airships weighs the longer it takes to reach the desired velocity.

In conclusion the airships mass has only a minor effect on the airships travel speed because the maximum velocity does not depend on the mass only on the acceleration.

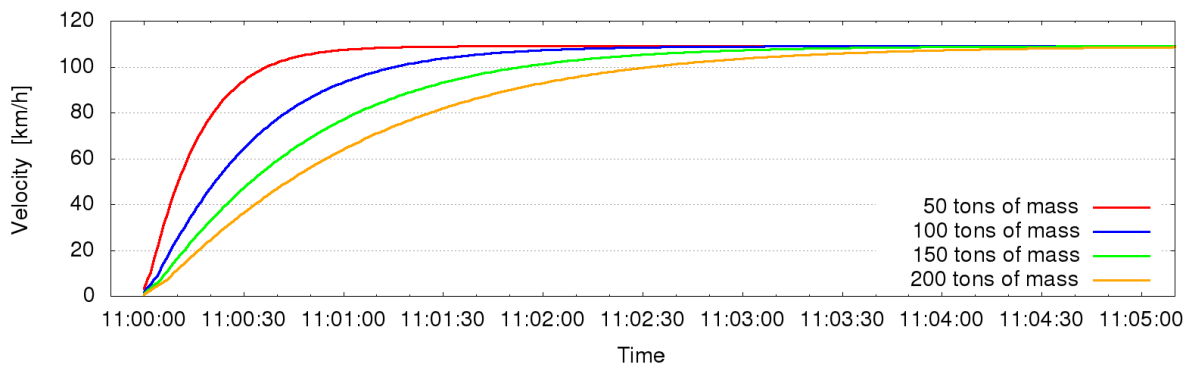


Figure 11: The velocity of the airship depending on its mass.

15.2 Results of center of mass check

An additional condition was, that the center of mass of an airship is lower than the center of geometry (CoG) of its envelope. In this simulation it is assumed, that the CoM which is 20 % of the airships maximum radius lower than the geometrical center is sufficient enough. In section 9.1 was the calculation of the CoM of the solar cell field explained. For an airship with solar cells all around the envelope the CoM is equal to the geometrical center of the hull ⁶. In case of a solar cells field on the top half of the 'Hindenburg' envelope the CoM of the field is 7.2 meter up above the airships hull's geometrical center. For the Zeppelin NT the CoM of the field is 2.5 meter above.

With these informations the the CoM of the entire airship can be calculated with the help of equation 21. The height and the mass of the solar cell field were explicit considered in the calculation. The values are listed in Table 10. The remaining parts, like engines or gondola are condensed in the value 'Remaining airship'. The CoM has to be 4.7 meter lower than the midpoint of the envelope for the 'Hindenburg' and 2.0 meter for the Zeppelin NT.

Table 10: Results and input parameter of the center of gravity evaluation.

-	'Hindenburg'		Zeppeling NT	
-	mass [$kg \cdot 10^3$]	height from CoG [m]	mass [kg]	height from CoG [m]
Solar cell field	5.3	7.2	0.56	2.5
Entire airship	113.6	-4.1	4.7	-1.4
Remaining airship	108.3	-4,7	4.2	-2.0

16 Simulation results

For the evaluation of the simulation in most cases the test track is located in Germany. The distance is from the Hamburg townhall (53.551,9.994) to the Viktualienmarkt in Munich city center (48.135, 11.574) in linear distance. The route has a distance of 612 km.

Some simulation parameter do vary for the evaluation. For example the altitude the flight level of the airship as well as if there are only solar cells on top of the airship or also on the bottom (compare 9.1). Further the date of the simulation and finally also the location do vary. In the last evaluation the airship will fly along various latitude and not the described route in Germany. The simulation also distinguish if wind data are included in the calculations. This is the case for flights near the ground with less than 150 meter of altitude. For the fixed input parameter consult Table 7 and 8 respectively 9.

⁶The gaps in the solar cell field caused by e.g. the gondola are neglected

16.1 Comparing the 'Hindenburg' and the Zeppelin NT

At first the simulation is to point out the differences between the introduced airships 'Hindenburg' and Zeppelin NT with a special interest in the different sizes of the solar cell fields. Therefore a time frame of a few minutes during the flight from Hamburg to Munich was chosen. The plot in Figure 12 shows the velocity of the airship on the abscissa and a time frame from 10:54 pm to 11:07 am on the ordinate.

The Zeppelin NT with a solar cell field covering the top half of the envelope reaches the lowest velocities, up to 105.5 km/h. The same airship with an envelope totally covered in solar cells reaches fastest velocities. In this scenario maximum 114.2 km/h.

The 'Hindenburg' with the setup of only one solar cell field on the top half on the contrary reaches a top speed of 109.7 km/h. In total, the highest velocities reaches the 'Hindenburg' with a value of 117.0 km/h. The double amount of solar cells increases the top speed in these scenarios for approximately 7 km/h.

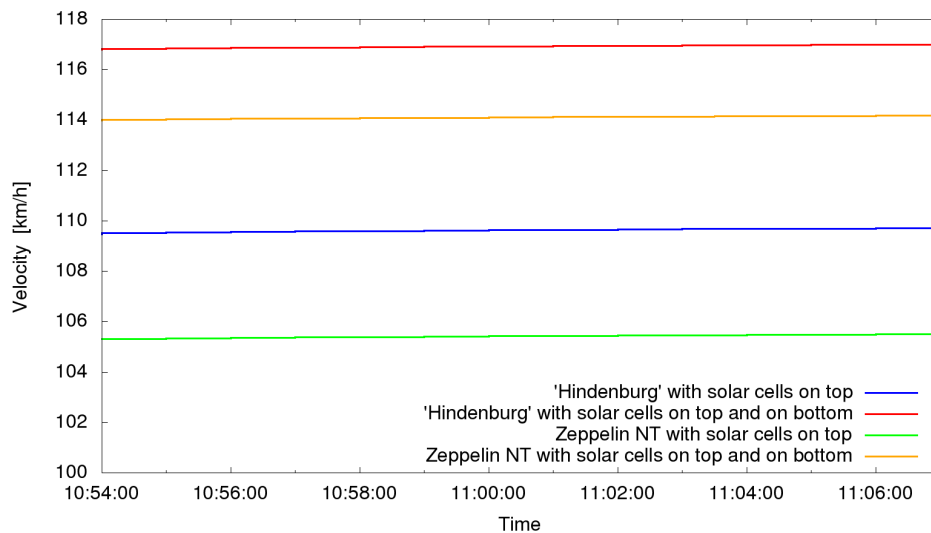


Figure 12: Comparison between the 'Hindenburg' and the Zeppelin NT.

In the remaining simulations the Zeppelin NT airship will be taken into account with a solar cell field only on the top half of the envelope. The reason is that this might be the most economically reasonable airship configuration.

16.2 The influence of the wind on the airship

The airship's envelope is a good target for the wind. This can be an advantage or disadvantage depending if the wind blows from behind or against the airships front. The importance of the wind impact should be observed with the help of Figure 13. In this scenario the Zeppelin NT solar airship travels from Hamburg to Munich on the 1th of

July in the year 2012 ⁷.

Two simulated flights are shown in the plot. The thin line represents the velocity of the airship with wind data and the thicker line the flight without using any wind data to compare. The ordinate shows the velocity in km/h and the ordinate the time span.

The highest differences between the two graphs are in time interval from 9 pm to 9:30 pm.

On one hand with tailwind a speedup of 10,2 km/h was accomplished at 9:14 pm and 9:16 pm. On the other hand at 9:11 pm the airship travels 8.5 km/h slower than in the reference flight without wind data (82.5 km/h with wind data and 91.0 km/h without wind data).

The corresponding windspeed is shown in Figure 14. The plot which has the same axis labeling shows the wind speed calculated from equation 82. The equation uses the tail respectively front wind proportion of the wind data records. The plot is structured in a way, that frontwind is listed as a positive velocity value and backwind as a negative. The reason of the described speedup is at 9:14 pm and 9:16 pm coursed a tailwind with speed approx. 14.5 km/h. The minor speed at 9:11 pm is due to a frontwind of approx. 13.2 km/h.

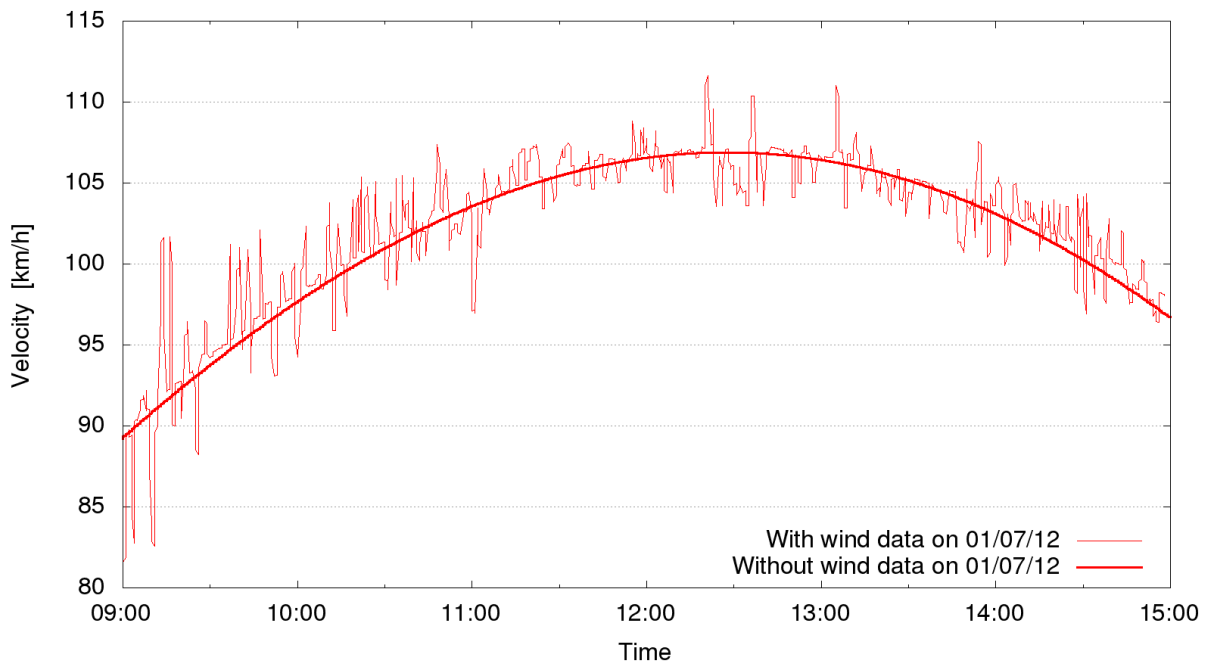


Figure 13: The influence of the wind at the airship.

⁷All weather data are from the year 2012 because this is the latest records in the German Weather Service Database.

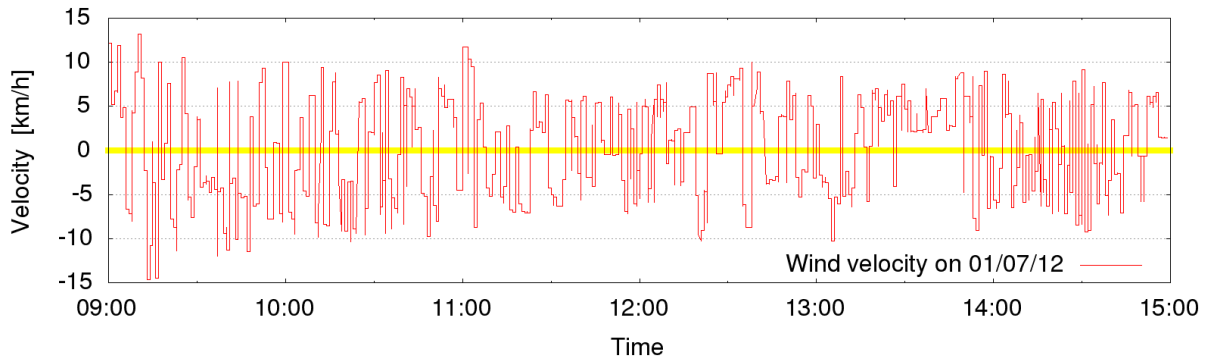


Figure 14: The wind velocity on the route.

In the appendix are similar flights of the Zeppelin NT on two additional days in order to simulate different wind scenarios. The date is always the first of the month in June, and August. The velocity of the Zeppelin NT on the 1st of June is shown in section C in Figure 21 and of 1st of August in Figure 23. The associated wind speed is shown in Figure 23 and Figure 24. A visualisation of the corresponding wind speed, wind direction, air pressure and temperature data in general of Germany at noon are also listed in the appendix in section C. Compare Figure 25 to 30 to make further investigations.

16.3 The influence of the altitude on the airships velocity

The calculation of the drag force in section 3 equation 6 pointed out the dependency from the air density. With rising flight altitude the density decreases and so does the drag force the airship has to overcome. In addition the thrust of the engines also depends on the air density. This was presented in section 10.

Figure 15 pictures the the flight of the Zeppelin NT airship from Hamburg to Munich with different flight levels on the 1st of August. The six graphs in the plot are showing the velocities from flights with 1 km to 6 km altitude in 1 km steps. The achieved velocities are increasing by increasing altitude. Flying on 6 km makes velocities possible up to almost 140 km/h. In the same time velocities of approx. 30 km/h less were traveled with the Zeppelin NT in a flight level of 1 km altitude.

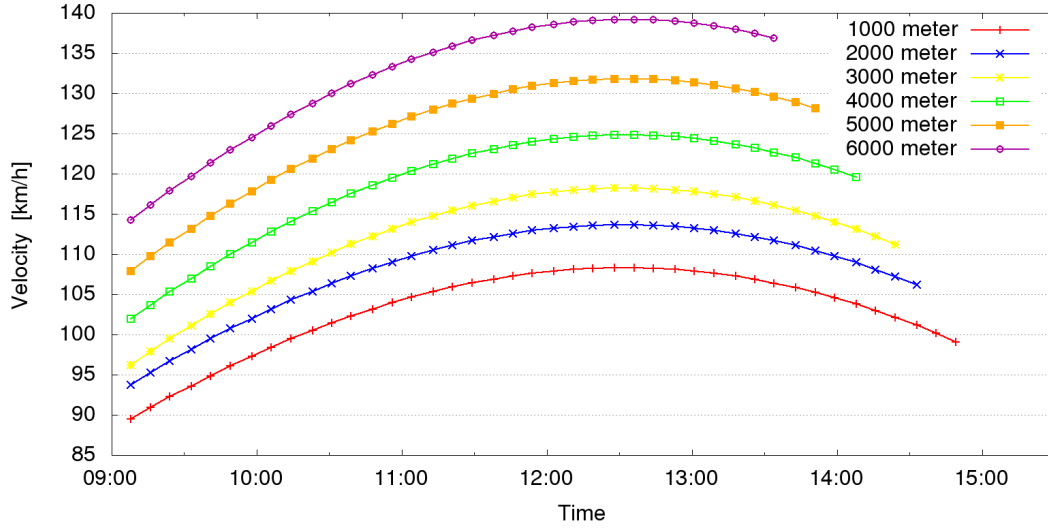


Figure 15: The velocity of the Zeppelin NT on different altitude.

The required respectively produced energy for the presented flights with different altitude is shown in Figure 16. The abscissa shows the produced power of the solar cell field in kilowatt and the ordinate again the time span.

It stands out, that the generated power increases evenly except for the power values of the 2 km and 3 km graph. The cause is the different power calculation. For altitude with more than 2.5 km the calculation of diffuse radiation has to be excluded and the simulation has to fall back on equation 39 to calculate the direct radiation. This was mentioned in section 8.5 and 8.6.

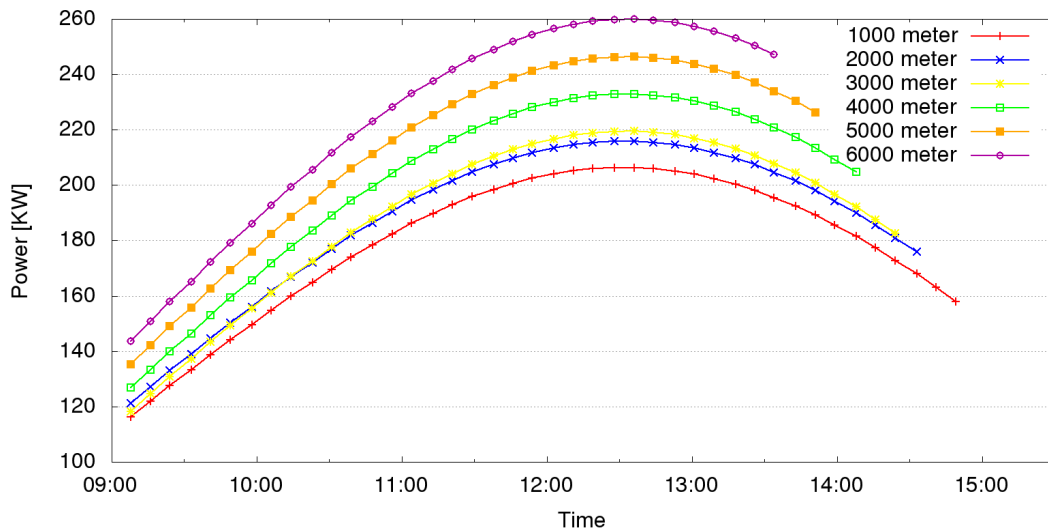


Figure 16: The generated power of the Zeppelin NT on different altitude.

Finally in Table 11, the average velocity, the maximum velocity and the flight duration

for the flights from Hamburg to Munich on different altitude is listed.

Table 11: Results of the Zeppelin NT flight on different altitude.

flight altitude [km]	1.0	2.0	3.0	4.0	5.0	6.0
average velocity [km/h]	102.7	108.0	112.0	118.4	125.0	131.8
maximum velocity [km/h]	108.3	113.6	118.2	124.8	131.8	139.2
duration [h:min]	5:57	5:40	5:27	5:10	4:53	4:38
distance [km]	612.0					

16.4 Simulation results for different seasons and locations

In this last evaluation chapter the Zeppelin NT travels along various latitudes in summer and winter. The goal is to figure out, the airship operating range and the velocity the airship can accomplish on ideal conditions. For the simulated track the Tropic of Cancer, as well as north and south europe was chosen. The corresponding latitude for the Tropic of Cancer is 23.5th and for europe 40th and 60th parallel north. The starting point for all simulations is the prime meridian. and the airship travels strictly in east direction, starting at 8:00 pm and finishing at 16:00 am. Additionally for the 40th and 60th parallel north an evaluation was made in winter on solstice the 21th of December. The date for the remaining simulations were the solstice in summer on 21th of June.

Two different flight levels were chosen, 1 km and 6 km.

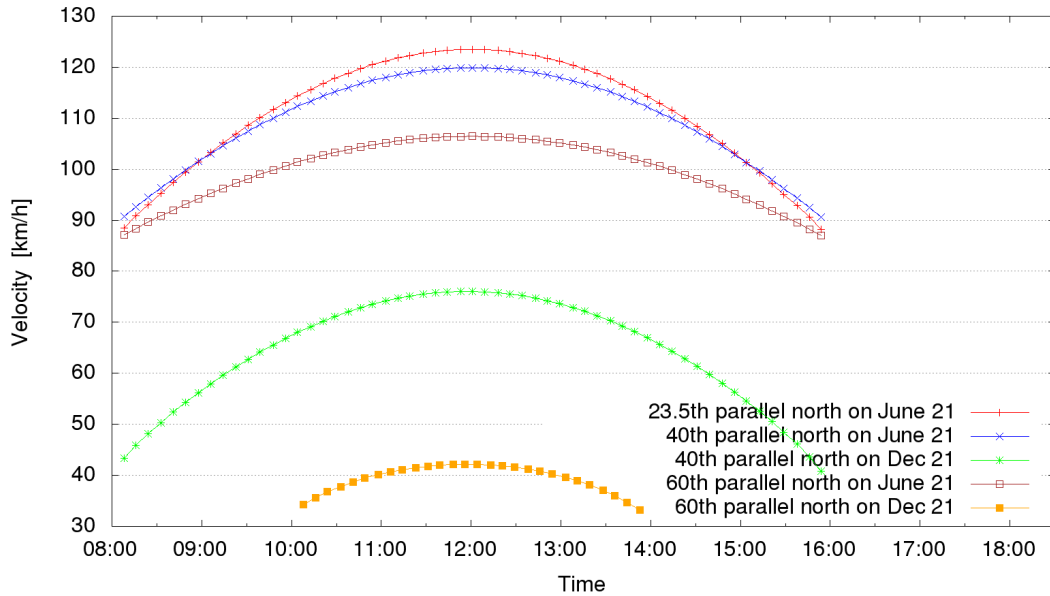


Figure 17: The airship velocity on flights with 1 km altitude on different locations.

Figure 17 shows the velocity for flights with 1 km altitude. The highest velocity was accomplished under optimal conditions on the Tropic of Cancer (23.5th parallel north).

On the 21.6 the sun reaches its zenith, therefore the maximum energy per square meter arrives on the earth's surface. This causes a Zeppelin NT velocity up to 123.5 km/h. A flight maximum velocity on the 40th parallel north is closely followed with 119.9 km/h. The simulations on the 21st December cannot reach velocities that fast. Flying on the 40th parallel after all accelerates up to 76.0 km/h. On the 60 degree of Latitude sunrise and sunset were before respectively after 8.00 pm and 16:00 am. Therefore only a 4 hours flight beginning at 10:00 pm were simulated. The maximum velocity was the lowest with 42.2 km/h.

Additionally in Figure 18 is the corresponding power in kilowatt, which the solar field is creating is outlined. All mean and maximum velocities are summarized in Table 12 as well as the accomplished distances and the required time.

Table 12: Results of the Zeppelin NT on flights with 1 km altitude on different locations.

Latitude (date)	23.5 (21.06)	40.0 (21.06)	40.0 (21.12)	60.0 (21.06)	60.0 (21.12)
Average velocity [km/h]	110.8	109.3	64.1	99.4	39.1
Maximum velocity [km/h]	123.5	119.9	76.0	106.5	42.2
Distance [km]	886.6	874.7	512.9	795.3	156.4
Duration [h:min]	8:00				4:00

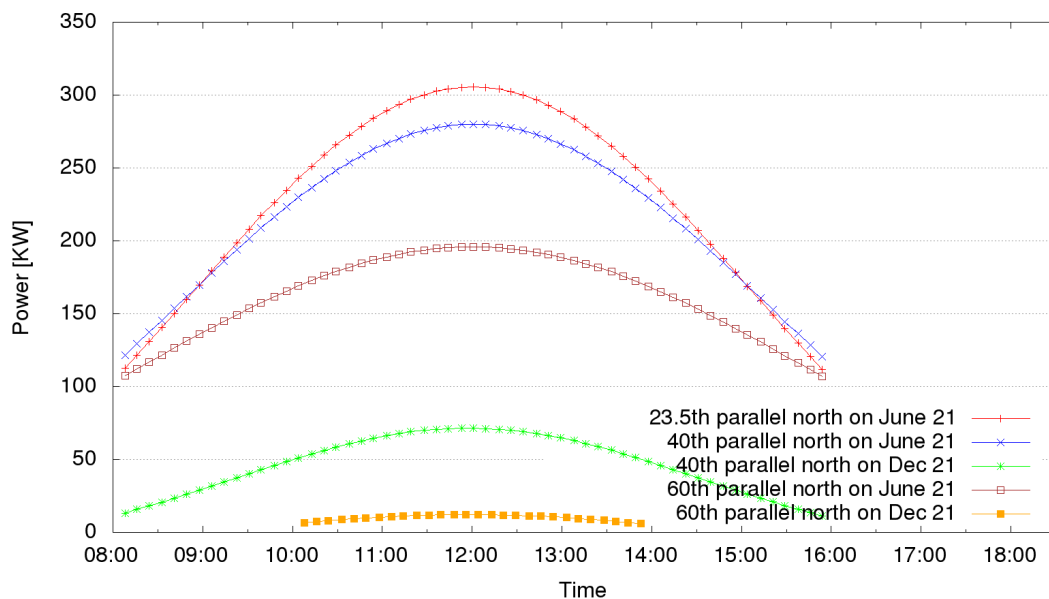


Figure 18: The generated power on flights with 1 km altitude on different locations.

A similar simulation was done with the difference of a flight level on 6 km altitude. In section 16.3 the increasing airship velocity by increasing altitude was already presented. The graphs in Figure 19 should again clarify the maximum velocity an airship can accomplish on ideal conditions.

The maximum velocity increases by 34.2 km/h to 157.7 km/h, the fastest computed velocity in this thesis. Further all velocities increased by the increasing altitude. For further information compare Figure 19 for a graphical visualisation and Table 13 for the exact results of mean and average velocity as well as the flight distance and duration. For plot with the produced energy during that flights compare Figure 20.

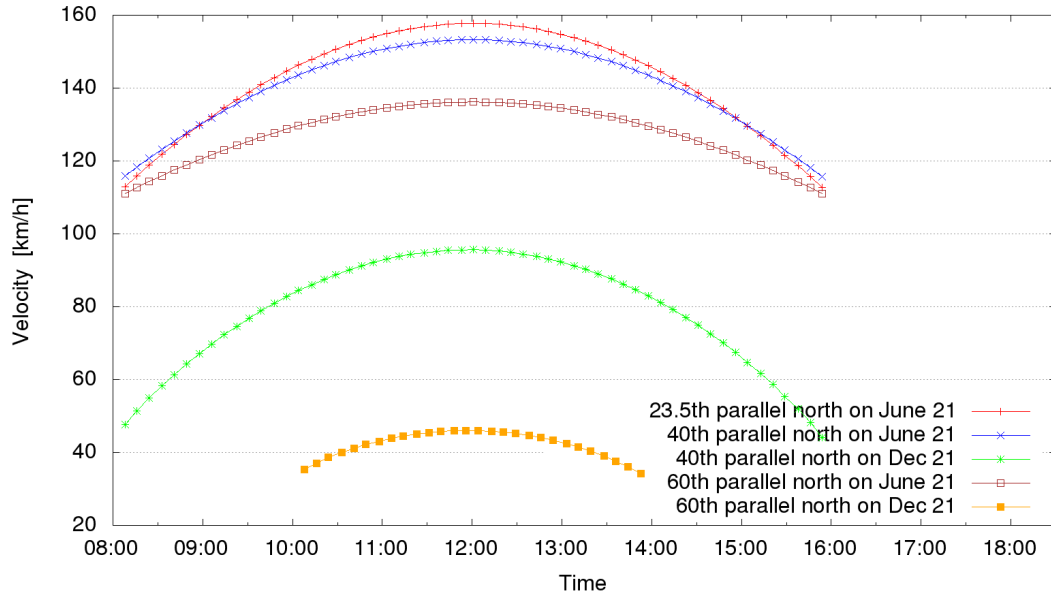


Figure 19: The airships velocities on flights with 6 km altitude on different locations.

Table 13: Results of the Zeppelin NT on flights with 1 km altitude on different locations.

Latitude (date)	23.5 (21.06)	40.0 (21.06)	40.0 (21.12)	60.0 (21.06)	60.0 (21.12)
Average velocity [km/h]	141.7	139.8	78.5	127.1	41.8
Maximum velocity [km/h]	157.7	153.3	95.6	136.2	46.0
Distance [km]	1133.24	1118.3	628.0	1016.7	167.3
Duration [h:min]	8:00				4:00

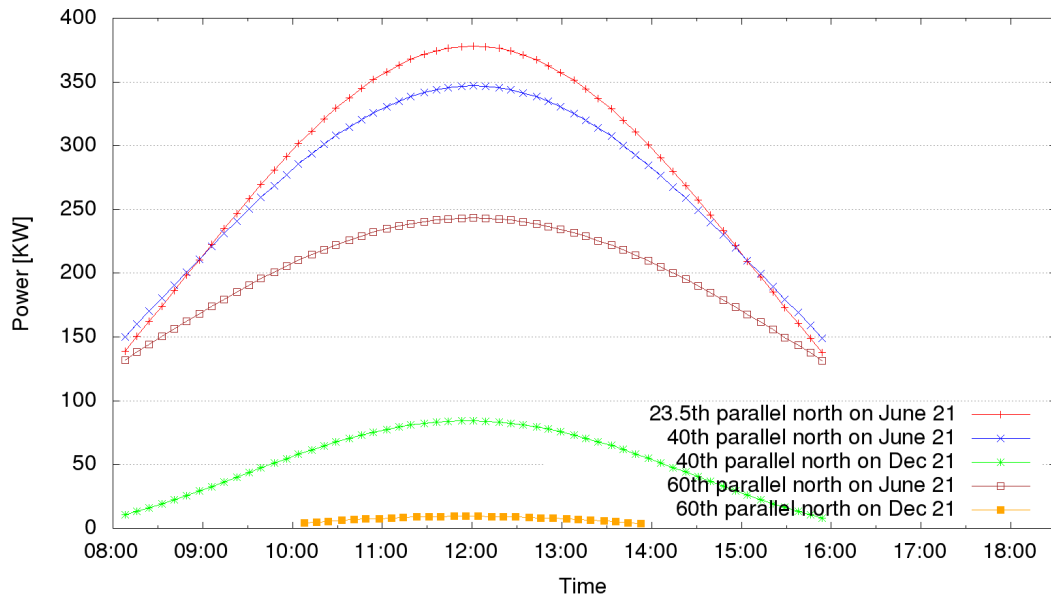


Figure 20: The generated power on flight with 6 km altitude on different locations.

17 Conclusion and future work

Various simulations with the 'Hindenburg' and especially the Zeppelin NT showed the performance capability of solar airships. Under the condition of different airship parameter settings like e.g. the flight altitude and the locations, the flight velocity was determined. Fortunately a solar airship can achieve under favorable conditions reasonable traveling velocities, to handle longer distances. Beyond that it would be possible to develop algorithms for optimizing flight routes in dependency of weather circumstances like advantageous wind directions on different flight levels.

A Input paramter for the evaluation of the efficiency of the engines

Table 14: Parameter for the efficiency of the engine.

Parameter	Value
v	$72 \frac{km}{h}$
d_{prop}	$2m$
F_{thrust}	$3000N$
P_{prop}	$100KW$
ρ	$1.225 \frac{kg}{m^3}$
n_{motor}	1

B Additional data for the buoyancy of the airships

Table 15: Remaining masses for various maximum altitude.

Max. altitude [km]	'Hindenburg' remaining mass [$kg \cdot 10^3$]	'Zeppelin NT' remaining mass [$kg \cdot 10^3$]
0	211.2	8.7
1	191.7	7.9
2	173.5	7.2
3	156.6	6.5
4	141.2	5.8
5	126.9	5.2
6	113.8	4.7
7	101.7	4.2
8	90.6	3.7

C Additional weather data simulation results

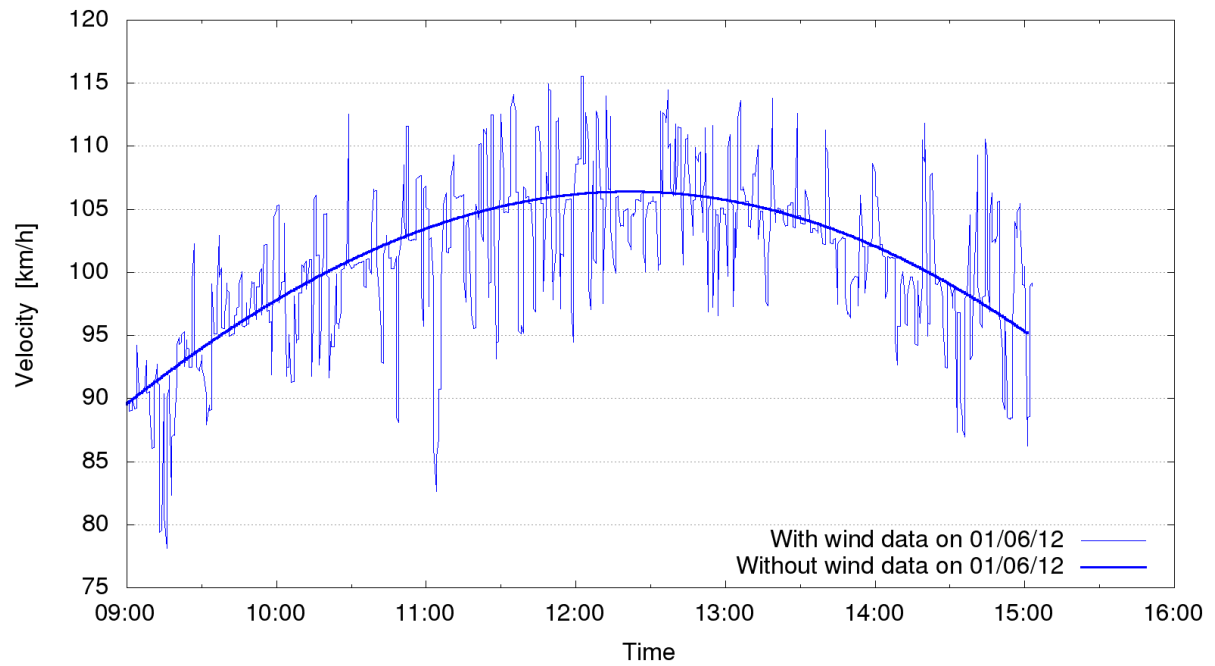


Figure 21: The influence of the wind on the airship.

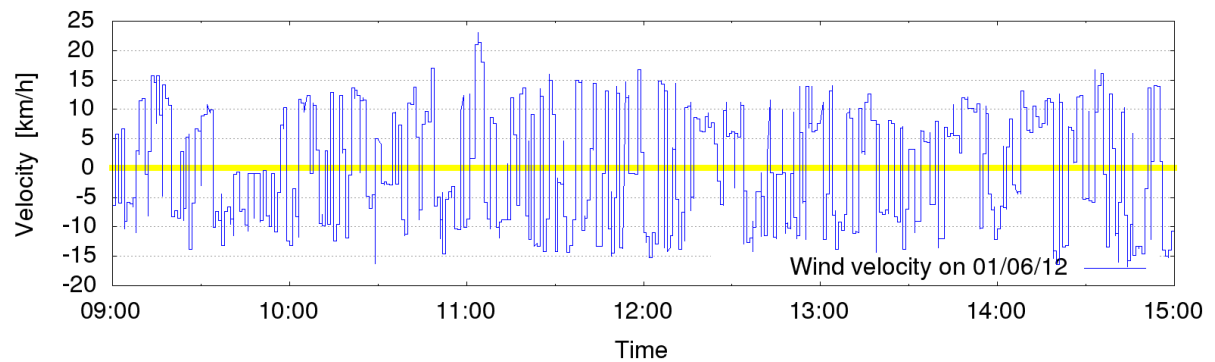


Figure 22: The influence of the wind on the airship.

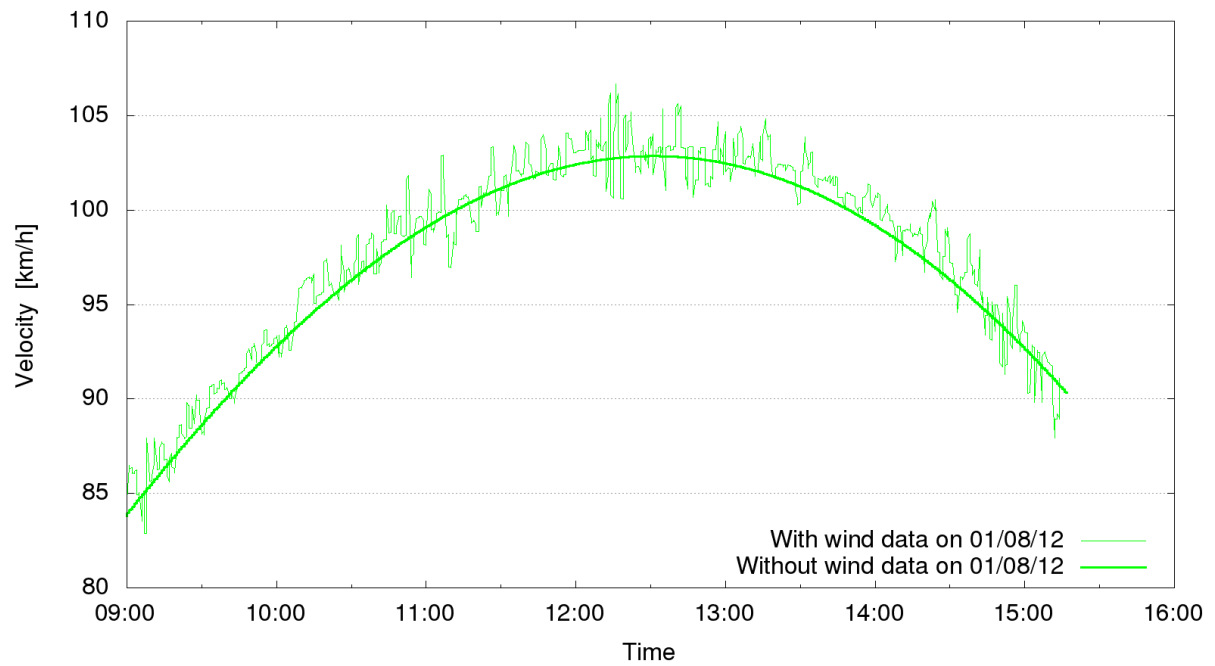


Figure 23: The influence of the wind on the airship.

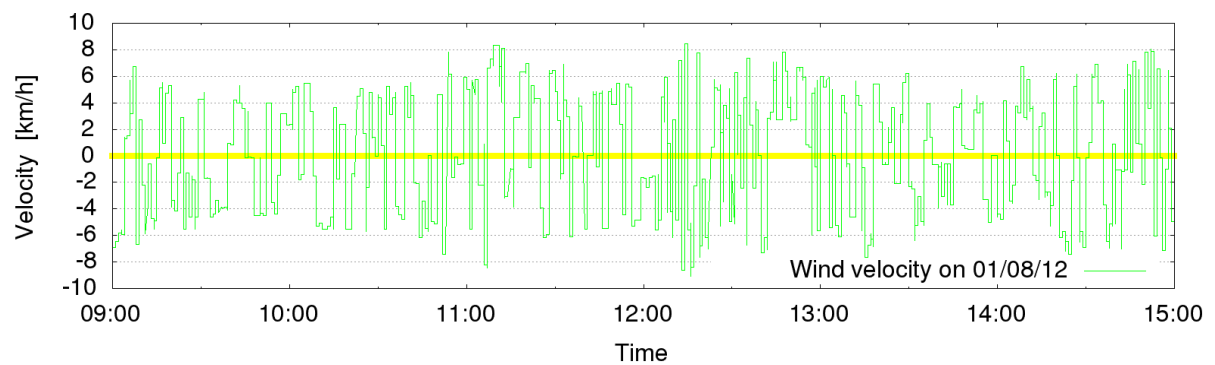


Figure 24: The influence of the wind on the airship.

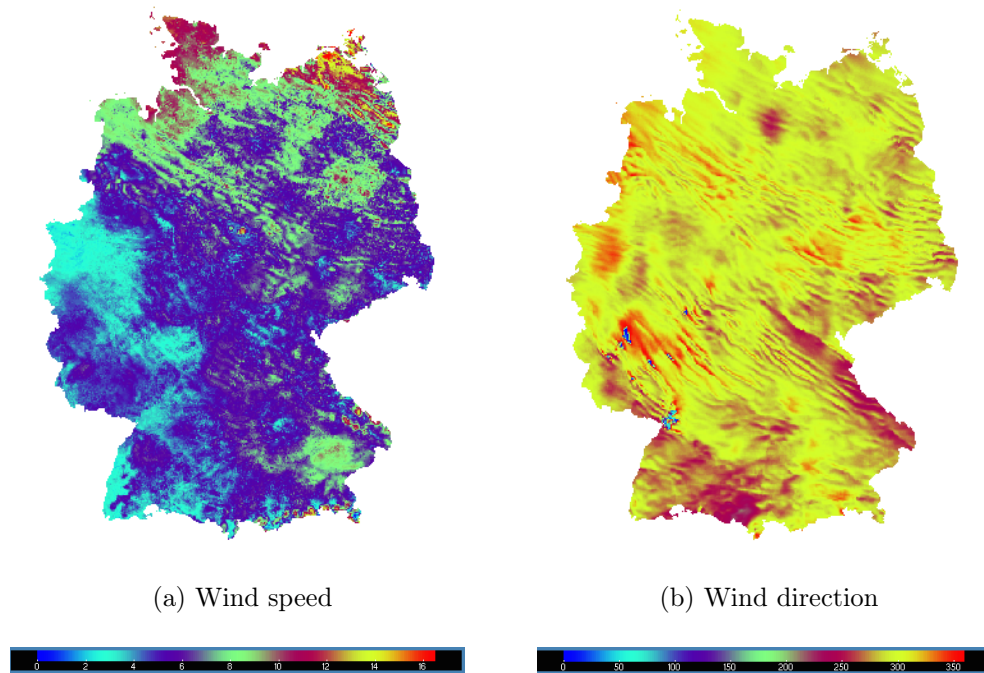
Weather data visualisation

Figure 25: Wind data at noon 01/06/12.

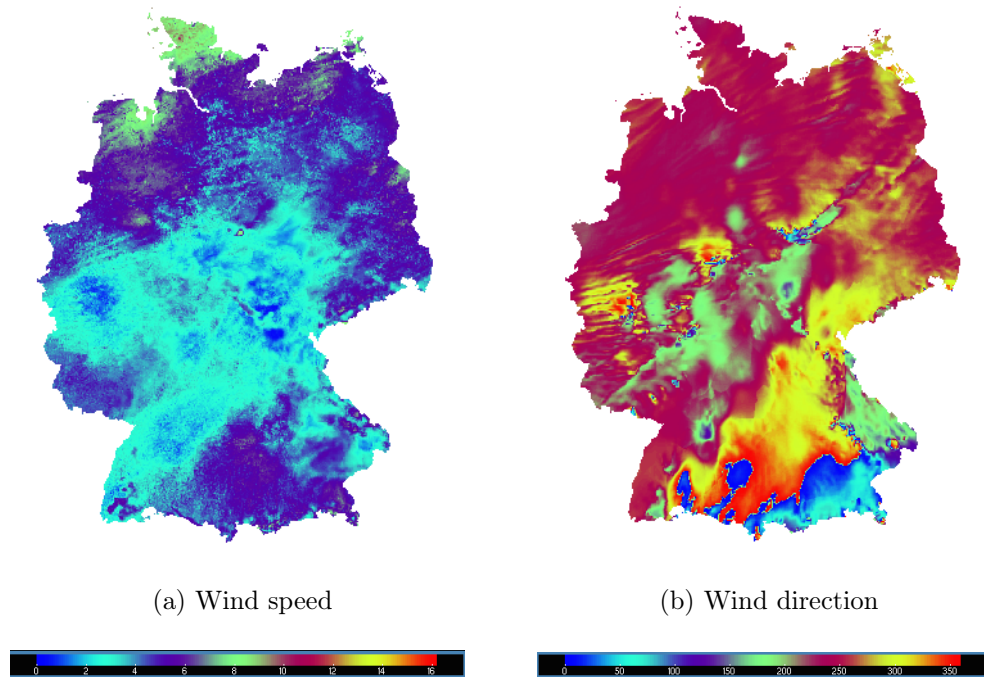


Figure 26: Wind data at noon 01/07/12.

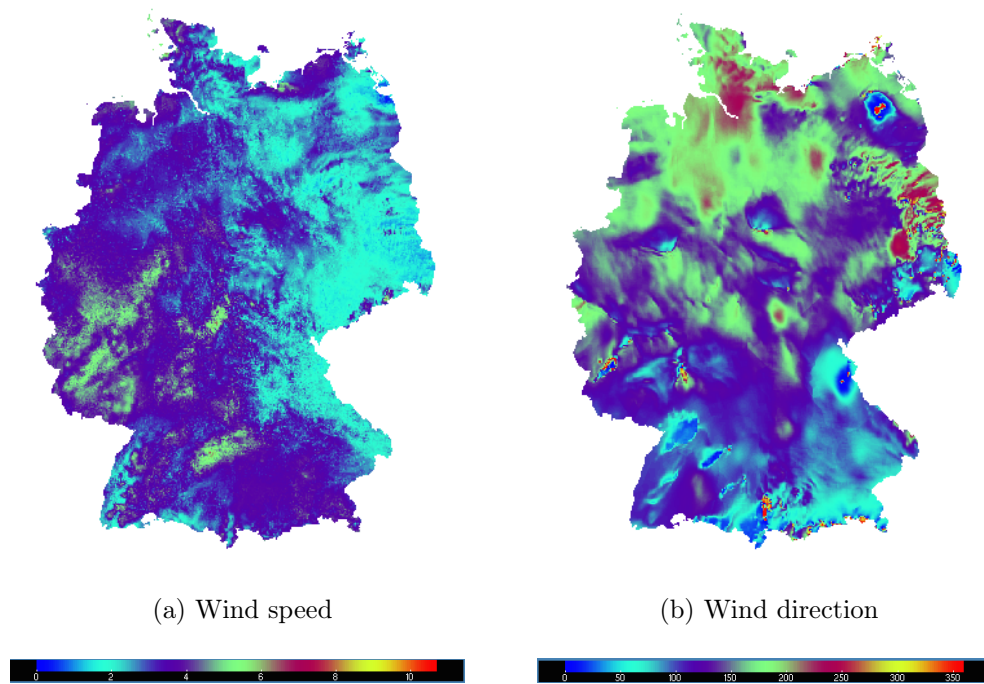


Figure 27: Wind data at noon 01/08/12.

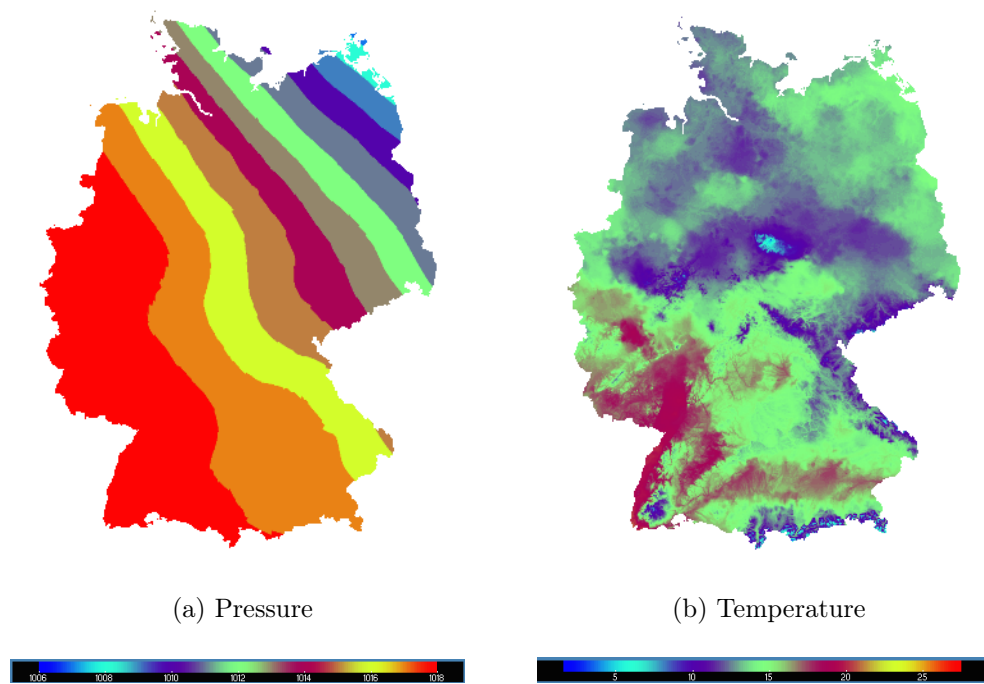


Figure 28: Pressure and temperature at noon 01/06/12.

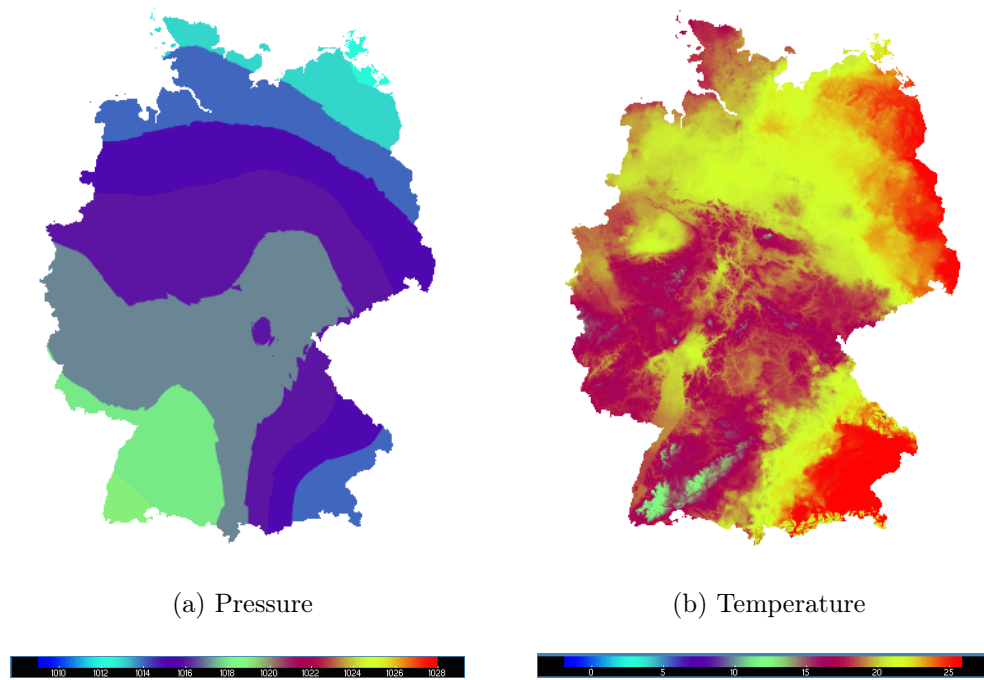


Figure 29: Pressure and temperature at noon 01/07/12.

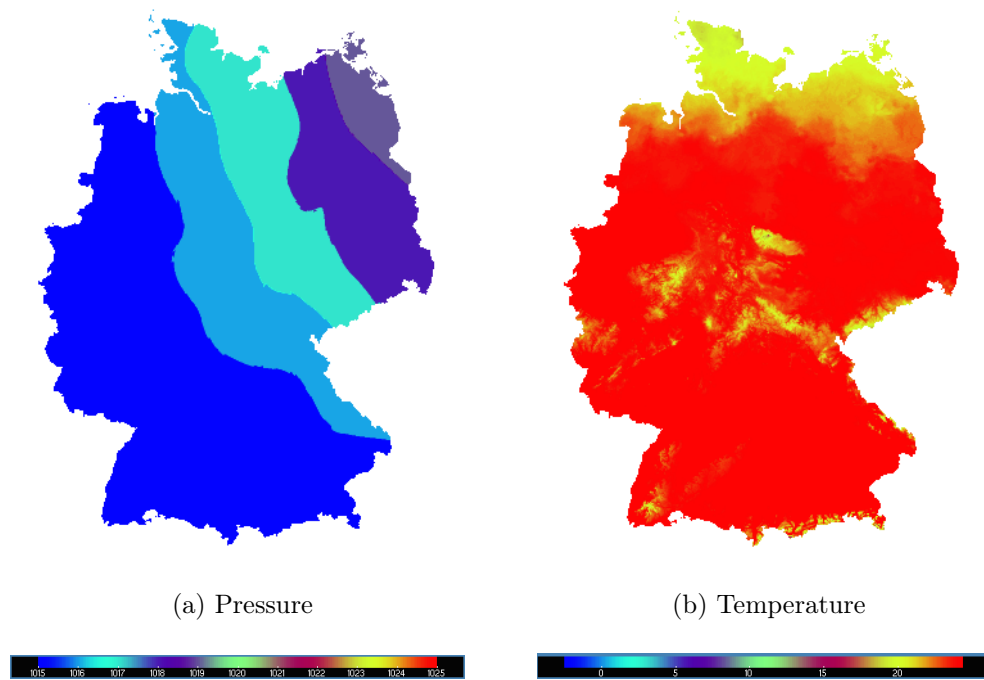


Figure 30: Pressure and temperature at noon 01/08/12.

D Literature

- [1] Goldson, Jordan. WWI Zeppelins: Not Too Deadly, But Scary as Hell. (2014) <https://www.wired.com/2014/10/world-war-i-zeppelins/> [21.12.2017].
- [2] Mueller, Joseph; Paluszek, Michael (2004) .Development of an Aerodynamic Model and Control Law Design for a High Altitude Airship. University of Minnesota, Minneapolis. Page 5f.
- [3] Ozoroski, Thomas; Mas, Kyle; Hahn, Andrew (2003). A pc-based design and analysis system for lighter -than-air unmanned vehicles. NASA Langley Research Center, American Institute of Aeronautics and Astronautics, San Diego, California Page 4.
- [4] U.S. Standard Atmosphere, U.S. Government Printing Office, Washington, D.C., 1976. Page 6. https://www.eoas.ubc.ca/books/Practical_Meteorology/prmet/PracticalMet_WholeBook-v1_00b.pdf [17.10.2017].
- [5] Duffie, John; Beckman, William (2013). Solar Engineering of Thermal Processes. 4th Edition, John Wiley & Sons Inc. Page 6ff.
- [6] Stull, Roland (2015). Practical Meteorology. First edition, Dept. of Earth, Ocean and Atmospheric Sciences University of British Columbia 2020-2207 Main Mall Vancouver, BC, Canada. Page 6.
- [7] Calculate distance, bearing and more between Latitude/Longitude points. <http://www.movable-type.co.uk/scripts/latlong.html> [20.10.2017].
- [8] Khoury, Gabriel (2013). Airship Technology. 2th Edition, Cambridge University Press. Page 522f.
- [9] Khoury, Gabriel (2013). Airship Technology. 2th Edition, Cambridge University Press. Page 161.
- [10] Khoury, Gabriel (2013). Airship Technology. 2th Edition, Cambridge University Press. Page 27.
- [11] Khoury, Gabriel (2013). Airship Technology. 2th Edition, Cambridge University Press. Page 525.
- [12] Leutenegger, Stefan; Jabas, Mathieu; Siegwart, Roland (2010). Solar Airplane Conceptual Design and Performance Estimation. Springer Science+Business Media B.V. Page 548.
- [13] Stull, Roland (2015). Practical Meteorology. First edition, Dept. of Earth, Ocean

- and Atmospheric Sciences University of British Columbia 2020-2207 Main Mall Vancouver, BC, Canada. Page 6.
- [14] Heinemann, Detlev; Behrendt, Tanja (2013). Energy Meteorology, 2th Edition, Carl von Ossietzky University of Oldenburg. 1th Edition. Page 50.
 - [15] Dobos, Endre (2013). Albedo, 2th Edition, University of Miskolc, Miskolc-Egyetemvaros, Hungary. Encyclopedia of Soil Science. DOI: 10.1081. Page 2.
 - [16] Duffie, John; Beckman, William (2013). Solar Engineering of Thermal Processes. 4th Edition, John Wiley & Sons Inc. Page 68.
 - [17] Duffie, John; Beckman, William (2013). Solar Engineering of Thermal Processes. 4th Edition, John Wiley & Sons Inc. Page 70.
 - [18] Maleki, Seyed; Hizam H.; Gomes Chandima (2017). Estimation of Hourly, Daily and Monthly Global Solar Radiation on Inclined Surfaces: Models Re-Visited. Energies 2017, 10, 134. Page 3.
 - [19] Drueck, Harald (2012). Solarthermie I (Teil 1) Manuskript zur Vorlesung. Institut fuer Thermodynamik und Waermetechnik (ITW). Page 17.
 - [20] Klein, William (1948) .Calculation of solar radiation and the solar heat load on man. Journal of metrology. Vol 5, No 4, 134. Page 122.
 - [21] Mueller, Joseph; Paluszek, Michael (2004) .Development of an Aerodynamic Model and Control Law Design for a High Altitude Airship. University of Minnesota, Minneapolis. Page 3f.
 - [22] Kaempfl, Bernhard (2004). Flugmechanik und Flugregelung von Luftschiffen. Institut fuer Flugmechanik und Flugregelung, Universitaet Stuttgart. Page 20ff.
 - [23] Bohl, Willi; Elmendorf, Wolfgang (1978). Technische Stroemungslehre. 3th edition. Vogel-Verlag. Page 79ff.
 - [24] Brüning, Gerhard; Hafer, Xaver; Sachs, Gottfried (1986). Flugleistungen, 2th Edition, Springer-Verlag Berlin Heidelberg. Page 60.
 - [25] K.L.S. Publishing. Der Propeller – das unverständene Wesen. <http://klspublishing.de/ejournals/e-Journ%20A1-05%20Der%20Propeller%20das%20unverstandene%20Wesen.pdf> [25.11.2017].
 - [26] File Transfer Protocol (FTP). J. Postel. <https://tools.ietf.org/html/rfc959> [22.11.2017].

- [27] Network Common Data Form (NetCDF). <https://www.unidata.ucar.edu/software/netcdf/> [22.11.2017].
- [28] Grossman, Dan. Hindenburg Statistics. <http://www.airships.net/hindenburg/size-speed/> [28.11.2017].
- [29] Hindenburg Design and Technology. <http://www.airships.net/hindenburg/hindenburg-design-technology/> [28.11.2017].
- [30] Vor 50 Jahren: Das Ende des Luftschiffs LZ 129 Hindenburg. H. Holtz. <http://www.deutsches-museum.de/fileadmin/Content/data/Insel/Information/KT/heftarchiv/1987/11-2-102.pdf> [8.12.2017].
- [31] Grossman, Dan. Zeppelin NT. <http://www.airships.net/zeppelin-nt/> [9.12.2017].
- [32] Windprofil-Rechner. <https://wind-data.ch/tools/profile.php> [11.12.2017].
- [33] Statista GmbH. Anteile der Bodenbedeckung in Deutschland im Jahr 2009. (2016) <https://de.statista.com/statistik/daten/studie/169661/umfrage/bodenbedeckung-in-deutschland-2009/> [29.12.2017].
- [34] <https://www.technologyreview.com/s/528351/record-breaking-solar-cell-points-th> [21.12.2017].
- [35] Rolf, Gloor. Elektromotoren. (2011) <http://www.energie.ch/elektromotoren> [21.12.2017].